



**INSTITUTO POTOSINO DE INVESTIGACIÓN
CIENTÍFICA Y TECNOLÓGICA, A.C.**

POSGRADO EN CIENCIAS EN BIOLOGIA MOLECULAR

**CHARACTERIZATION OF THE RESPONSE OF *Candida
glabrata (Nakaseomyces glabratus)* CLINICAL
ISOLATES TO NEUTROPHILS**

Tesis que presenta

Ana Belén Vargas Antillón

Para obtener el grado de

Maestra en Ciencias en Biología Molecular

Director (Codirectores) de la Tesis:

Dra. Irene Beatriz Castaño Navarro

Dra. Ma. Guadalupe Gutiérrez Escobedo

San Luis Potosí, S.L.P., junio de 2024



Constancia de aprobación de la tesis

La tesis “**Characterization of the response of *Candida glabrata* (*Nakaseomyces glabratus*) clinical isolates to neutrophils**” presentada para obtener el Grado de Maestra en Ciencias en Biología Molecular fue elaborada por **Ana Belén Vargas Antillón** y aprobada el **día de mes de año** por los suscritos, designados por el Colegio de Profesores de la División de Biología Molecular del Instituto Potosino de Investigación Científica y Tecnológica, A.C.

Dra. Irene Beatriz Castaño Navarro

Dra. Ma. Guadalupe Gutiérrez Escobedo

Dra. Ana María Estrada Sánchez



Créditos Institucionales

Esta tesis fue elaborada en el Laboratorio de Laboratorio de Microbiología Molecular de la División de Biología Molecular del Instituto Potosino de Investigación Científica y Tecnológica, A.C., bajo la dirección de las doctoras Dra. Irene B. Castaño Navarro, apoyada por el proyecto CF-2019 No. 610281 y la Dra. Ma. Guadalupe Gutiérrez Escobedo.

Durante la realización del trabajo el autor recibió una beca académica del Consejo Nacional de Ciencia y Tecnología (No. 1241696) y del Instituto Potosino de Investigación Científica y Tecnológica, A. C.

Acta de Examen

Dedicatorias

A MIS PADRES, ROSALBA Y MARTIN, NO SOLO POR GUIARME POR EL CAMINO DE LA VIDA, SINO TAMBIÉN EN MI TRAYECTORIA PROFESIONAL, POR AYUDARME A SER MEJOR PERSONA CADA DÍA, POR DAR LO MEJOR DE USTEDES A LA DISTANCIA PARA QUE YO LLEGARA HASTA AQUÍ, ES GRACIAS A USTEDES QUE SIEMPRE ENCUENTRO MI CAMINO.

A MI HERMANA ANDREA, POR SIEMPRE ABRIRME LAS PUERTAS DE SU CASA CUANDO VOY DE VISITA Y SER UN EJEMPLO PARA MÍ COMO MUJER PROFESIONAL.

A MI HERMANO ALEXYS, POR SUS PALABRAS DE ALIENTO DURANTE TODO ESTE PROCESO E INSPIRARME A SER PERSEVERANTE Y DEDICADA.

A ROGELIO, POR SER ESA PERSONA QUE SIEMPRE CREE EN MÍ, POR ESTAR EN TODO LOS MOMENTOS BUENOS Y MALOS, TE ADORO.

UN DÍA PROMETÍ QUE TODOS LOS TRIUNFOS QUE ESTUVIERAN POR VENIR EN MI FUTURO SERIA PARA USTEDES, Y ESTA NO ES LA EXCEPCIÓN.

CON CARIÑO:

BELENCHO.

Agradecimientos

Este trabajo me ha permitido explotar mi capacidad intelectual, enriquecerme de conocimientos, experiencia y por permitirme desarrollar dentro de un laboratorio de investigación científica, además de darme cuenta de todo lo que soy capaz y aprenderme a valorar. Esto fue gracias el apoyo de muchas personas a las cuales quiero agradecer en este apartado.

Al Instituto Potosino de Investigación Científica y Tecnológica por el apoyo institucional, así como la formación académica.

Al Laboratorio Nacional de Biotecnología Agrícola, Médica y Ambiental, por permitirme estar en sus instalaciones para la realización de experimentos.

Al Consejo Nacional de Humanidades, Ciencias y Tecnologías (Conhacyt) por el apoyo económico brindado para ser posible la realización de mis estudios.

Mi más grande agradecimiento a la Dra. Irene Castaño Navarro, por su dedicación, paciencia, valiosa asesoría, enseñanza y apoyo tanto académico como personal, por ser ese ejemplo de maravillosa persona y una fuerte motivación para mí como mujer científica. Irene, gracias por ser como eres.

Al Dr. Alejandro de las Peñas, por sus ideas, sugerencias y enseñanzas durante este proyecto, además de las pláticas que trajeron alegría y risas durante este proceso.

Un agradecimiento especial a la Dra. Ma. Guadalupe Gutiérrez Escobedo, por su trabajo y apoyo técnico. Sin duda alguna, su enseñanza de igual manera fue una fuerte motivación y un ejemplo para mí como científica.

A la Dra. Ana María Estrada Sánchez por sus comentarios y apoyo.

Al Dr. Nicolás Gómez Hernández y Dr. Saul Jijón Moreno por su apoyo técnico.

A Rogelio Morales, por los neutrófilos donados para ser posible esta tesis.

A Gloria López, porque además de ser la chispa de L6, su labor brindada en el laboratorio es crucial para nosotros.

A Emily y compañeros de Laboratorio 6, en especial a Grecia, Laura, Mariana y Alex, por brindarme su amistad y enseñanza. Agradezco infinitamente por coincidir con ustedes, por las risas en los días tristes y estresantes, por las palabras de aliento y apoyo incondicional. Un placer compartir tanto con ustedes, los quiero mucho.

A Renato y Diego, por siempre, siempre brindarme su apoyo incondicional, por estar para mí en todo momento, no sé qué haría sin ustedes.

A Valeria Torres Sánchez, por ser, por estar, por existir. Te quiero y adoro demasiado.

Finalmente, a los Vargas, por celebrar mis triunfos como si fueran suyos, los amo incondicionalmente.

Index

Constancia de aprobación de la tesis	ii
Créditos Institucionales	iii
Acta de Examen	iv
Agradecimientos	vi
Index	vii
Figures List	ix
Tables List	xi
Abreviaturas	xii
Resumen	xiii
Abstract	xiv
Introduction	1
Materials and methods	4
Preparation of <i>N. glabratus</i> strains.	4
Purification of NØ.	4
Microevolution of <i>N. glabratus</i> strains.	4
Survival assay.	5
Growth rates.	5
Media.	6
Spot assay.	6
Reversibility assay.	6
Yeast transformation.	7
Construction of mutants in the BG14 strain genetic background.	7
Statistical Analysis.	7
Results	7
Microevolution in the standard strain BG14.	7
Percentage of petite cells obtained after exposure to NØ (Survival assay).	11
The growth rate of evolved strains in CAA.	11
Three consecutive passes through NØ may decrease chronic H ₂ O ₂ exposure of <i>N. glabratus</i> .	13
Microevolution in <i>N. glabratus</i> clinical isolates.	15
Phenotypic characterization of the surviving <i>N. glabratus</i> clinical isolates.	19
<i>N. glabratus</i> mutants in histone deacetylases are involved in survival to NØ attack.	22
Phenotypic characterization of the surviving <i>N. glabratus</i> knockout mutants.	24
Discussion	27
Consecutive passages through NØ do not enhance resistance to NØ.	27
<i>N. glabratus</i> mutants <i>rdp3Δ</i> and <i>hos2Δ</i> are involved in the survival against NØ.	28
Gcn5 is not involved in the survival to NØ.	29

The epigenetic response participates in different types of stress.	29
References	32
Supplementary material	36
Supplementary tables.	36
Table S1 Strains generated.	36
Table S2 Primers.	40
Table S3 Program fusion PCR.	41
Table S4 Percent reversibility of Gly ⁻ to Gly ⁺ phenotype.	41
Supplementary Figures.	43
Fig. S1 Schematic representation of experimental approach.	43
Fig. S2 Schematic representation spot assay with different oxidant stresses, antifungals and thermal stress.	44
Fig. S3 Schematic representation of reversibility assay.	45
Fig. S4 Schematic representation of the experimental approach of fusion PCR.	46

Figures List

- Fig. 1| Survival assay. Reference strain was exposed two hours to NØ (BG14); NØGly⁻ and NØGly⁺ colonies, were exposed to NØ for three passes (six hours) the phenotype was observed, and cells were stored at -80°C, cells were recovered and immediately exposed again to fresh NØ two more hours (eight hours in total) for the survival assay. As controls, Gly⁺ and Gly⁻ colonies were exposed as above for six hours to RPMI medium (RPMI Gly⁺ and RPMI Gly⁻ respectively) cells were stored at -80°C, recovered and exposed to NØ for two hours for the survival assay. Difference between groups was assessed by Ordinary one-way ANOVA followed by Tukey's multiple comparisons post-hoc test according to data normality. P-values ≤0.05 were considered statistically significant n=3. 10
- Fig. 2| Spot assay under different oxidative stress types and fluconazole. Abbreviations Ch: Gly⁻ phenotype colonies, Gr: Gly⁺ phenotype colonies, FLC: fluconazole, MEN: menadione, H₂O₂: hydrogen peroxide, INPUT: colonies without stress conditions, Rn: technical replicate. Strain CGM1938 is a Gly⁻ strain derived from treatment of BG14 with ethidium bromide. The differences between columns 1 and 2 versus 4 is the number of passes: columns 1 and 2 have 3 passes through NØ plus a survival assay and column 4 has three passes through NØ. 14
- Fig. 3| Survival assay in *N. glabratus* clinical isolates after 3 (2-hour) passages through NØ. a) Parental strains, exposure to NØ for two h (survival assay) n=3, b) Percent survival after 6 h exposure to NØ n=1 (three passes through NØ) AN376: % survival of parental strain; AN378: % survival of parental strain; AN376 6h: three consecutive passages of two h each through NØ, six h in total; AN378 6h: three consecutive passages of two h each through NØ, six h in total. c) Survival assay of strains recovered after the 6 h exposure to NØ (eight hours total exposure): AN376: % survival of parental strain; AN376 8h: three consecutive passages of two h each through NØ, plus one survival assay, eight h in total; CGM5217 and CGM5218: colonies derived from AN376 with eight h exposure in total n=3. d) AN378: % survival of parental strain; AN378 8h: three consecutive passages of two h each through NØ, plus one survival assay, eight h in total; CGM5219 and CGM5220 colonies derived from AN378 with eight h exposure in total n=3. Difference between groups was assessed by Ordinary one-way ANOVA followed by Tukey's multiple comparisons post-hoc test according to data normality. P-values ≤0.05 were considered statistically significant. 16
- Fig. 4| Spot assay under different oxidative stress types and fluconazole of the *N. glabratus* clinical isolates. Abbreviations FLC: fluconazole, CSP: caspofungin, H₂O₂: hydrogen peroxide, BG14: reference strain. AN376: clinical isolates strain, CGM5217: isolated colony of AN376 strain after six h of exposure to NØ with small colony phenotype, CGM5218: regular colony size originated from the AN376 after six h to NØ, CGM5219: isolated colony of AN378 strain after six h of exposure to NØ with regular colony phenotype, CGM5220: small colony size originated from the AN378 after six h to NØ. n=3 21
- Fig. 5| Survival assay in *N. glabratus* knockout mutants after 2-hour passages through NØ. The difference between groups was assessed by Ordinary one-way ANOVA followed by Turkey's multiple comparisons post-hoc test according to data normality (**p* < 0.05). P-values ≤0.05 were considered statistically significant n=3. 23
- Fig. 6| Spot assay under different oxidative stress conditions and fluconazole of the histone acetylation/deacetylation knockout mutants. Abbreviations FLC: fluconazole, CSP: caspofungin, H₂O₂: hydrogen peroxide, BG14: reference strain. *hos2Δ*: recovered strain, 1: regular size colony isolated of *hos2Δ* strain after two h of exposure to NØ, 2: regular colony size originated from *hos2Δ* after two h to NØ, *gcn5Δ*: recovered glycerol strain, 1: regular size

colony isolated of *gcn5Δ* strain after two h of exposure to NØ, *rpd3Δ*: recovered glycerol strain, 1: regular size colony isolated of *rpd3Δ* strain after two h of exposure to NØ. n=2 26

Tables List

Table 1 Percentage of petite cells obtained after a 2 h exposure to NØ	9
Table 2 Growth curve in synthetic complete medium of BG14 under different treatments	12

Abreviaturas

CAA	Casamino Acids
CSP	Caspofungin
CFUs	Colony Forming Units
FLC	Fluconazole
HATs	Histone acetyltransferase
HDACs	Histone desacetylase
H₂O₂	Hydrogen Peroxide
MEN	Menadione
NETs	Neutrophils Extracellular Tramps
NØ	Neutrophils
OD	Optical Density
ON	Overnight
PAMPs	Pathogen-associated Molecular Patters
PRRs	Pattern Recognition Receptors
ROS	Reactive Oxygen Species
RPMI-H-S	RPMI-HEPES-SERUM
YPD	Yeast Extract Peptone Dextrose
YPG	Yeast Extract Peptone Glycerol

Resumen

Las infecciones por patógenos fúngicos están aumentando debido al incremento de la población inmunocomprometida. Algunos de los patógenos fúngicos más comunes del género *Candida* adquieren resistencia a los antifúngicos durante los procesos de infección. *N. glabratus* no solo muestra una resistencia alta a los antifúngicos, sino que también tiene una susceptibilidad relativamente baja a los neutrófilos (NØ). Esto se debe, en parte, a que *N. glabratus* provoca una respuesta inflamatoria de baja intensidad mientras se desplaza silenciosamente dentro del huésped. Como resultado, la activación de los NØ se retrasa, lo que permite al patógeno evadir eficazmente la respuesta inmune.

Dado que *N. glabratus* puede evadir el sistema inmune y resistir parcialmente el ataque de los NØ, evaluamos si existe una microevolución de *N. glabratus* cuando se expone repetidamente de manera secuencial a los NØ.

Utilizamos la cepa estándar del laboratorio de *N. glabratus* (BG14) y dos aislados clínicos diferentes que son resistente (AN378) o susceptible (AN376) a fluconazol (FLC), el antifúngico más comúnmente usado, para exponerlos secuencialmente a NØ y, posteriormente, recuperar las células sobrevivientes. Caracterizamos varios fenotipos de las células que sobrevivieron, incluyendo la disfunción mitocondrial (fenotipo Gly⁻), tiempos de duplicación y supervivencia a una nueva exposición a NØ. Además, para determinar si la acetilación/desacetilación de las histonas participan en la supervivencia a los NØ, construimos mutantes en 2 acetilasas (HATs) y dos desacetilasas de histonas (HDACs) HATs y HDACs y evaluamos su supervivencia a los NØ.

No observamos un aumento en la supervivencia después de tres exposiciones consecutivas a los NØ. Demostramos por primera vez que las HDACs Rpd3 y Hos2 están involucrados en la supervivencia a NØ, mientras que la HAT Gcn5 no participa en esta respuesta.

Palabras clave: *N. glabratus*, neutrófilos, acetilasa de histona, deacetilasa de histona, aislados clínicos, supervivencia.

Abstract

Infections by fungal pathogens are increasing due to a rise in the immunocompromised population, some of the most commonly found fungal pathogens of the *Candida* genus acquire resistance to antifungals during the infection of the host. *N. glabratus* is characterized by a relatively low susceptibility to neutrophils (NØ), effectively evading the immune response due to the induction of a low-grade inflammatory response by silently transiting within the host, leading to a delay in neutrophil activation.

Since *N. glabratus* can evade the immune system and partially resist NØ attack, we determined if there is microevolution of *N. glabratus* when serially exposed to NØ that results in mutants or epigenetic variants which confers higher survival to neutrophil.

We used our standard laboratory *N. glabratus* strain (BG14) and two different clinical isolates of which one is resistant (AN378) and the other susceptible (AN376) to fluconazole (FLC), the most commonly used antifungal, to sequentially expose them three consecutive times to NØ. Afterwards, we recovered the surviving *N. glabratus* cells and tested them further for several phenotypes including mitochondrial function (Gly⁻ phenotype), growth rates and survival to a new exposure to fresh NØ. To determine whether histone acetylation/deacetylation participates in survival to NØ, we constructed mutants of histone acetylases (HATs) and deacetylases (HDACs) and their survival to NØ was evaluated.

Three passes through NØ did not increase the resistance to NØ in the *N. glabratus* clinical isolates or the BG14 strain. We demonstrated for the first time that the HDACs *Rpd3* and *Hos2* are involved in *N. glabratus* survival to NØ, whereas *Gcn5* is not.

Key words: *N. glabratus*, neutrophils, histone acetylase, histone deacetylase, clinical isolates, NØ survival.

**CHARACTERIZATION OF THE RESPONSE OF *Candida glabrata*
(*Nakaseomyces glabratus*) CLINICAL ISOLATES TO NEUTROPHILS**

Key words: *N. glabratus*, neutrophils, histone acetylase, histone deacetylase,
clinical isolates, survival percentage.

Ana-Vargas¹, Ma. Guadalupe-Gutierrez¹, Irene-Castaño¹

¹División de Biología Molecular, Instituto Potosino de Investigación Científica y
Tecnológica. Camino a la Presa San José 2055, San Luis Potosí, S. L. P 78216,
Tel. (444) 0834 2038

* Corresponding author:

Dr. Irene Castaño

Mailing address: Camino a la Presa San José #2055. División de Biología Molecular
Instituto Potosino de Investigación Científica y Tecnológica. San Luis Potosí, San
Luis Potosí

78216, México

Phone (52) 444-834-2000 ext. 2038

Fax: (52) 444-834-2010

e-mail: icastano@ipicyt.edu.mx

Introduction

1
2 Infections by fungal pathogens are increasing, in part due to a rise in the
3 immunocompromised population, which turns these infections into a problem of
4 public health. Several species of *Candida*, such as *Candida glabrata* (*N. glabratus*),
5 have dramatically increased in prevalence as causes of bloodstream infections,
6 partly due to their high intrinsic and acquired resistance to antifungals (Pais et al.,
7 2019). It has been described that the main mechanism of antifungal acquired
8 resistance in *N. glabratus* is due to mutations that confer gain of function (GOF)
9 within the *PDR1* gene, resulting in upregulation of the efflux pumps Cdr1, Cdr2,
10 Snq2, and Qdr2, increasing drug expulsion (De las peñas et al., 2015; Pais et al.,
11 2019; Siscar-Lewin et al., 2021).

12 In addition to its high resistance to fungicides, *N. glabratus* is characterized by a
13 relatively low susceptibility to neutrophils (NØ), effectively evading the immune
14 response (Pais et al., 2019; Urban and Backman, 2020). As the first line of defense,
15 NØ play a crucial role in fighting/preventing infections caused by opportunistic fungal
16 pathogens through active recruitment to infected tissues and organs (Urban and
17 Backman, 2020).

18 According to reports, the recruitment and swarming of NØ to the site of infection is
19 the most common defense against fungi. However, it should be noted that other
20 mechanisms have also been described. NØ are part of the innate immunity, which
21 recognizes pathogen-associated molecular pattern molecules (PAMPs) through
22 pathogen recognition receptors (PRRs) (Ermert et al., 2009; Shantal et al., 2022;
23 Urban and Backman, 2020). Upon recognition of fungal ligands, signaling results in
24 phagocytosis, the release of cytokines and chemokines, and production of reactive
25 oxygen species (ROS), and neutrophil extracellular traps (NETs) (Ermert et al.,
26 2009; Shantal et al., 2022; Urban and Backman, 2020). Furthermore, a study
27 reported that NØ are capable of expelling *N. glabratus* cells after intracellular killing,
28 through a mechanism called “dumping”, highlighting this expulsion as an opportunity
29 for other immune cells to ingest fungal cells, present antigens and activate the
30 adaptive immune response (Essig et al., 2015).

31 However, *N. glabratus* owes its success to the establishment and persistence in the
32 host through the induction of a low-grade inflammatory response by silently transiting
33 within the host, leading to a delay in neutrophil activation (Shantal et al., 2022).
34 Likewise, the development of strategies such as evading phagocytosis and escape
35 to the cytosol, decreasing the production of proinflammatory cytokines, and
36 promoting internalization into non-phagocytic cells achieving its reproduction inside
37 of the mononuclear phagocytes has led to speculation that survival capacity is due
38 to multiple mechanisms such as antioxidant response, combined with the ability to
39 modulate the pH of the phagosome, which in part explain its ability to survive
40 phagocytosis and in fact to take advantage of the immune cells to succeed and
41 persist in the host (Shantal et al., 2022; Siscar-Lewin et al., 2021). Overall, the
42 increase in *N. glabratus* infections and its ability to evade the immune response
43 emphasizes the importance of timely neutrophil activation to trigger immune
44 response to fight potential opportunistic mycosis. This could result in future
45 strategies to treat severe fungal infections.

46 Previously, our research group found that *N. glabratus* survival to NØ attack depends
47 on cellular mechanisms induced by oxidative stress to maintain the appropriate
48 redox balance *N. glabratus*. We demonstrated that peroxiredoxin Tsa1 and Tsa2,
49 and the double mutant of catalase Cta1 with sulfiredoxin Srx1 are involved in
50 neutrophil survival, since the absence of these proteins leads to a 50% reduction in
51 survival compared to the parental strain BG14. Furthermore, we also showed that
52 the thioredoxin (Trx)/ thioredoxin reductases (Trr) system is necessary for NØ
53 survival, as mutants lacking these systems had 10% survival compared to the
54 parental BG14 (Gutiérrez-Escobedo et al., 2023). Finally, null mutants *hst1Δ* and
55 *sum1Δ* showed no difference in survival compared to BG14 (Vázquez-Franco et al.,
56 2022).

57 Increasing evidence suggests that epigenetic regulation plays a crucial role in
58 drug resistance (Lin et al., 2023; Pfaller et al., 2009; Yu et al., 2022). Histone
59 acetylation and deacetylation are post-translational modifications essential for
60 transcriptional regulation in eukaryotic organisms (Lin et al., 2023; Pfaller et al.,
61 2009; Yu et al., 2022). Histone acetylation levels involve two enzyme families:

62 histone acetyltransferases (HATs) and histone deacetylases (HDACs), which add or
63 remove acetyl groups from histone tails, respectively. Gcn5 is a HAT that forms part
64 of the SAGA (Spt-Ada-Gcn5-Acetyltransferase) complex catalytic subunit (Filler et
65 al., 2021; Lin et al., 2023; Yu et al., 2022). Among HDACs, Rpd3 is known for its role
66 in transcriptional regulation and silencing as a subunit of the Rpd3L complex, while
67 Hos2 is a NAD-dependent histone deacetylase and a subunit of both the Set3 and
68 Rpd3L complexes (Filler et al., 2021; Pfaller et al., 2009). The activity of these
69 modified histones has been implicated in resistance to various antifungals, cell wall
70 disruptors, and virulence in *N. glabratus* (Filler et al., 2021; Lin et al., 2023; Pfaller
71 et al., 2015; Wang et al., 2002; Yu et al., 2022). However, it remains uncharacterized
72 whether *N. glabratus* clinical isolates and reference strains can be induced to evolve
73 *in vitro* by exposure to NØ and whether these histone acetyltransferases and
74 deacetyltransferases are involved in the response and survival to NØ attack.

75 In this study, we demonstrated that consecutive passages through NØ do not
76 exhibit microevolution in terms of increased survival of *N. glabratus* strains against
77 NØ. Moreover, these passages do not confer greater resistance to various stresses
78 such as FLC or hydrogen peroxide (H₂O₂), but rather to temperature. Furthermore,
79 we observed that mutants in genes involved in histone deacetylation (*rpd3Δ* and
80 *hos2Δ*) display lower survival to NØ compared to the parental strain BG14, indicating
81 the involvement of epigenetic mechanisms in the response and survival to NØ
82 exposure, at least for histone deacetylation. Additionally, these mutants reveal
83 different phenotypes with respect to temperature sensitivity and resistance to FLC.

84

85

Materials and methods

86 **Preparation of *N. glabratus* strains.**

87 Yeast cells (BG14, AN376 and AN378) were grown to stationary phase (48 h
88 at 30 ° C with agitation) in 5 mL of yeast extract-peptone-dextrose (YPD). The optical
89 density (OD) was determined, and the cells were centrifuged and resuspended in 1
90 mL of sterile milli-Q water after which the OD₆₀₀ was measured and set at 1
91 (approximately 2x10⁷ per mL).

92 **Purification of NØ.**

93 Fifteen mL of venous blood from healthy volunteers was carefully mixed with
94 EDTA (final concentration 1.5-2 mM) and 15 mL of polymorphprep. The cell
95 suspension was centrifuged at 500 g for 35 minutes without using brake or
96 acceleration (to avoid lysis of NØ). The plasma and mononuclear cells were removed
97 and the lower band corresponding to NØ was harvested. The volume of NØ
98 suspension was diluted 1:1 with solution B (5 mM HEPES, 0.425% NaCl) and mixed.
99 The suspension was centrifuged at 400 g for 10 min with slow braking and
100 acceleration (setting 5). The pellet was resuspended in 4 mL of solution C (10 mM
101 HEPES, 0.83% NH₄Cl) and incubated for 10 minutes at 37°C with 5% CO₂ and
102 centrifuged at 400 g for 10 minutes. The pellet was resuspended in 4 mL RPMI-
103 HEPES-SERUM (RPMI-H-S) (1% Serum, 10 mM HEPES in RPMI), and finally, the
104 cells were counted in a Neubauer chamber and adjusted to 2.10⁶ cells/mL.

105 **Microevolution of *N. glabratus* strains.**

106 Neutrophil susceptibility assay was made following the original protocol
107 published by Ermet (2009) with the following modifications: (Gutiérrez-Escobedo et
108 al., 2020).

109 Three hundred µL of NØ cell suspension were placed in three wells of a 24-well
110 plate. As controls, 300 µL of RPMI-H-S were placed in 3 different wells and incubated
111 at 37°C with 5% CO₂ for 10 min. 30 µL of the yeast suspension was added to the
112 three wells that already contained NØ and to the three wells with only RPMI, and the
113 plate was centrifuged at 400 g for 10 minutes. The suspensions were incubated for

114 two hours at 37°C with 5% CO₂. Yeast cells were recovered by scraping and
115 reincorporated into a new well with fresh NØ. The exposure to NØ and RPMI-H-S
116 steps was repeated three times (to fresh NØ and RPMI-H-S). The contents of each
117 well were washed with 100 µL of cold, sterile milli-Q water, which caused lysis of the
118 NØ. Then, *N. glabratus* cells were frozen in 15% glycerol and stored at -80°C after
119 the last passage (for the clinical isolates AN376 and AN378, the cells were stored at
120 4°C after the last passage).

121 **Survival assay.**

122 *N. glabratus* cells were thawed and recovered in liquid YPD for two overnights (ON)
123 and the survival assay was performed again at 37°C with 5% CO₂ for two hours. The
124 contents of each well were collected in a new well and 100 µl of cold sterile milli-Q
125 water were added to lyse NØ. Each sample was diluted down to 10⁻³ and seeded
126 on YPD plates and incubated for 48 hours at 30°C (Fig. S1). Finally, the Colony
127 Forming Units (CFUs) were counted, and the survival percentage was determined
128 with the following formula (Ermet et al., 2019):

$$129 \quad \% \text{ survival} = \frac{\text{dilution factor (df)} \times \text{CFU (with neutrophils)} \times 100}{130 \quad \text{df} \times \text{CFU (without neutrophils)}}$$

131 **Growth rates.**

132 The doubling times of different *N. glabrata* strains were made following the protocol
133 published by: (Gutiérrez-Escobedo et al., 2023).

134 To determine the doubling times of BG14, CGM1938 (Gly^r generated with
135 ethidium bromide) and cells obtained after exposure to RPMI or NØ, cultures were
136 grown for 48 h in YPD, SC – Ura minimal medium or – amino acids media (CAA)
137 and diluted into their corresponding media. 2 × 10⁵ cells/mL were transferred to
138 multi-wells plates (Oy Growth Curves Ab ltd) containing 300 µL of fresh media. Cells
139 were grown at 30°C and monitored in a Bioscreen C system (Oy Growth CurvesAb
140 ltd) at OD_{450-580nm} every 15 min for 48 h. Doubling times were calculated in the
141 exponential growth phase as $dT = \ln_2 / (\ln OD_2 - \ln OD_1) / (t_2 - t_1)$. dT is doubling time,
142 OD1 is initial optical, OD2 is final optical density, t1 is initial time and t2 is final time.
143 Experiments were done in technical replicates. For statistical analysis, ANOVA two-

144 way test was performed using InStat Graph Pad software (InStat Graph Pad Inc., v.
145 8.0. San Diego, CA, USA). Standard deviations $p < 0.05$ was considered statistically
146 significant.

147 **Media.**

148 Yeast were grown in YPD medium containing 10 g/L yeast extract, 10 g/L
149 peptone, and supplemented with 2% glucose. Synthetic complete medium
150 composition: 1.7 g/L yeast nutrient base. 5 g/L $(\text{NH}_4)_2\text{SO}_4$ and supplemented with
151 0.6% casamino acids and 2% glucose. Yeast extract-peptone-glycerol (YPG)
152 medium contains 10 g/L yeast extract, 10 g/L peptone and supplemented with 3% of
153 glycerol (non-fermentable) carbon source where cells with non-functional
154 mitochondria cannot grow (Gly⁻ phenotype). To prepare YPD plates with selective
155 pressure, media were supplemented with FLC, caspofungin (CSP), H_2O_2 , tert-butyl
156 hydroperoxide or menadione.

157 **Spot assay.**

158 Dilutions of surviving *N. glabratus* cells were made in a 96-well plate. Each
159 sample was diluted down to 10^{-1} , 10^{-2} , 10^{-3} , 10^{-4} and 10^{-5} and spotted onto YPD
160 plates with different concentrations of FLC ([4,8,16, 32,42 and 64 mg/mL]), tert-butyl
161 hydroperoxide ([400, 800, 1200 and 1600 mM]), menadione ([30, 60 and 90 μM]),
162 and H_2O_2 ([5, 10, 15 and 20 mM]) and for thermal stress cells were spotted onto YPD
163 plates which were then incubated at 30°C, 37°C, 42°C, 45°C. Cells were grown for
164 48 hours and then plates were photographed at 24 and 48 hours (Fig. S2).

165 **Reversibility assay.**

166 To test the stability of the phenotypes obtained after the microevolution
167 experiment, nine consecutive subcultures in YPD medium were carried out by
168 inoculating 5 μL of an overnight culture of the Gly⁻ strain into 5 mL of fresh YPD
169 (medium without selective pressure). This procedure was repeated after
170 approximately 12 h and repeated consecutively until nine subcultures were
171 completed. After the last subculture, the tubes were incubated at 30°C until the
172 medium reached saturation, at which point the OD_{600} was measured, and cells were
173 adjusted to 1. Serial dilutions were made from 10^{-1} to 10^{-4} . One hundred microliters

174 of the 10⁻² and 10⁻³ dilutions were plated on YPG agar plates, while 100 microliters
175 of the 10⁻⁴ dilution were plated on YPD agar plates (Fig. S3).

176 **Yeast transformation.**

177 Yeast transformations were carried out with the product obtained from the fusion
178 PCR (full knock-out cassette) using the LiOAc/ssDNA/PEG method (Castaño et al.,
179 2003).

180 **Construction of mutants in the BG14 strain genetic background.**

181 Primers were designed with ApE software using the CBS138 reference genome;
182 for the 5' intergenic region primer, we used the complementary sequence of primer
183 #604 (used to amplify the *URA3* selection maker) and for the 3' intergenic region,
184 the complementary sequence of primer #605 (Primers are shown in Table S2).
185 Modules were made by PCR and the full knock-out cassette was obtained by fusion
186 PCR. Two steps were necessary for the fusion, the first step consisted of only 10
187 cycles using the 5' and 3' cassettes and the *URA3* selection marker. The second
188 step was performed in 20 cycles using the corresponding primers (Table S2) to
189 amplify the complete cassette (Fig. S4, Table S1).

190 **Statistical Analysis.**

191 Data distribution was evaluated by D'Agostino-Pearson normality test. Variables with
192 parametric distribution were reported as mean ± standard deviation. Differences
193 between intergroup comparisons were performed using analysis of variance
194 (ANOVA) followed by Turkey or Dunn's multiple comparisons post-hoc test,
195 according to data normality. Analyses were carried out using GraphPad Prism 8.0.1
196 (GraphPad Software Inc., San Diego, CA). For all tests, $p \leq 0.05$ was considered
197 statistically significant.

198 **Results**

199 **Microevolution in the standard strain BG14.**

200 We induced of microevolution of *N. glabratus* clinical isolates and reference
201 strains by repeated exposure to NØ *in vitro*.

202 Cells were exposed consecutively to NØ and RPMI medium for three 2-h
203 passages (Fig. S1a). Subsequently, cells were recovered for two ON and a survival
204 assay was performed again at 37°C with 5% CO₂ for two hours (Fig. S1b).

205 After the treatments, we obtained cells that formed small colonies compared to
206 the normal size of most of the colonies from strain BG14. This could be due to the
207 appearance of cells called petite, which form small colonies that are unable to use
208 non-fermentable carbon sources such as glycerol or ethanol due to mitochondrial
209 dysfunction.

210 We determined the percentage of petite colonies obtained after three passages
211 through NØ and one survival assay (Table 1).

212 No significant differences were found in the percentage of petites between the
213 strains; however, a higher proportion of petite colonies was observed in BG14 after
214 exposure to NØ

INITIAL STRAIN PHENOTYPE	# PREVIOUS PASSES	% PETITE (Gly ⁻)	WITHOUT TREATMENT
BG14 Gly ⁺	0	4.80±2.62 %	2.5%
NØ Gly ⁺	3	2.86±1.03 %	
RPMI Gly ⁺	0	2.91±1.08 %	

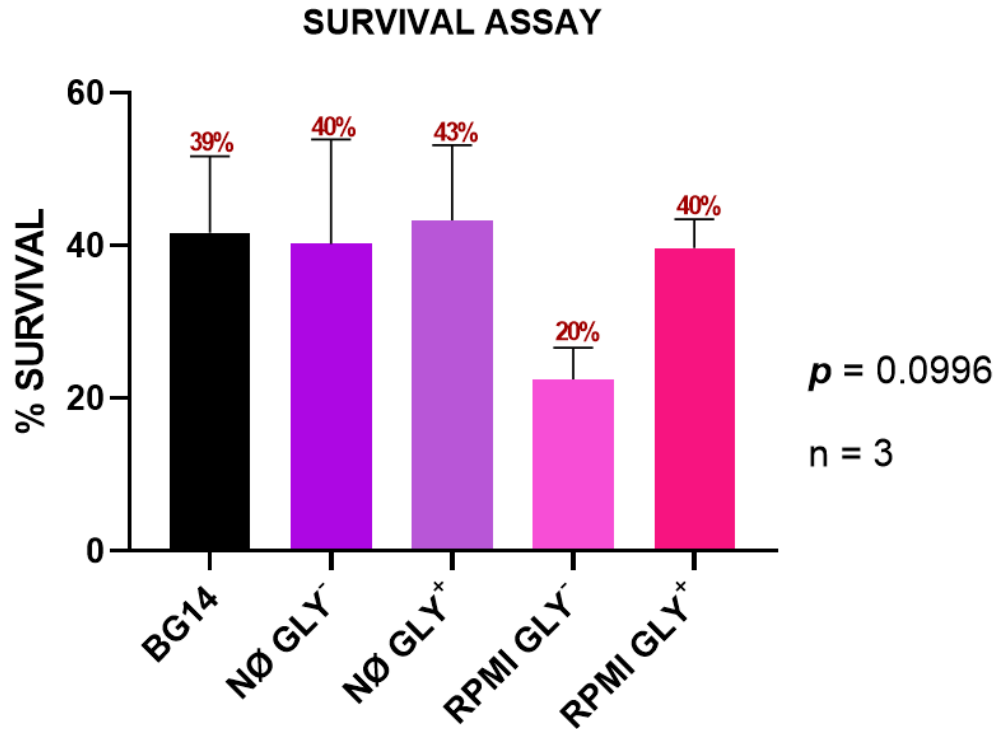
215 **Table 3|** Percentage of petite colonies obtained after a 2 h exposure to NØ. Abbreviations: BG14
216 Gly⁺: BG14 strain under phagocytosis conditions (one survival assay). NØ Gly⁺: BG14 strain under
217 phagocytosis conditions (three previous passes through NØ plus one survival assay). RPMI Gly⁺:
218 BG14 strain under RPMI medium conditions plus one survival assay. Data shows no differences
219 between them. Data are shown as mean ± s.d for parametric data. Difference between groups was
220 assessed by Ordinary one-way ANOVA test for parametric data. P values ≤ 0.05 were considered
221 statistically but no differences were found. Data represents the mean of 6 technical replicates, n=2.
222

223 We then asked whether *N. glabratus* can be induced to microevolved to NØ
224 resistance by repeated exposure to NØ.

225 Cells were exposed to NØ and RPMI medium for three passages every two hours
226 and then frozen at -80°C, Subsequently the cells were recovered for two ON and the
227 survival assay was performed again at 37°C with 5% CO₂ for two hours, to determine
228 whether previous repeated exposure to NØ, resulted in higher neutrophil survival
229 rates.

230 Although there are no significant differences in the survival rates of cells
231 recovered from the different treatments, there is a slight increase in survival trends
232 for Gly⁺ cells repeatedly exposed to NØ Gly⁺ (43%) compared to the strain (BG14)
233 without exposure to NØ (39%). However, no difference was observed in the survival
234 rate of NØ Gly⁻ (40%) compared to the absence of treatment. On the other hand, a
235 lower survival trend was observed in cells treated with RPMI for the Gly⁻ (20%) and
236 Gly⁺ (40%) derivatives, compared to BG14, although these differences are not
237 statistically significant.

238 Even though differences are not statistically significant, lower survival trends are
239 observed in cells with Gly⁻ phenotype previously exposed to RPMI medium (Fig. 1).



240

241 **Fig. 1| Survival assay. Reference strain was exposed two hours to NØ (BG14);** NØGly⁻ and
 242 NØGly⁺ colonies, were exposed to NØ for three passes (six hours) the phenotype was observed, and
 243 cells were stored at -80°C, cells were recovered and immediately exposed again to fresh NØ two
 244 more hours (eight hours in total) for the survival assay. As controls, Gly⁺ and Gly⁻ colonies were
 245 exposed as above for six hours to RPMI medium (RPMI Gly⁺ and RPMI Gly⁻ respectively) cells were
 246 stored at -80°C, recovered and exposed to NØ for two hours for the survival assay. Difference
 247 between groups was assessed by Ordinary one-way ANOVA followed by Tukey's multiple
 248 comparisons post-hoc test according to data normality. P-values ≤0.05 were considered statistically
 249 significant n=3.

250 **Percentage of petite cells obtained after exposure to NØ (Survival assay).**

251 We then asked whether the percentage of colonies with a Gly⁻ phenotype in strain
252 BG14 increases after the stress condition compared to the no-stress condition.

253 After repeated exposure to NØ for three consecutive passages, we performed a
254 survival assay by exposing these *N. glabratus* cells to NØ at 37 ° C with 5% CO₂ for
255 two hours. *N. glabratus* cells were diluted down to 10⁻³, plated on YPD plates,
256 incubated for 24 hours at 30°C and then, we determined CFUs and recorded the
257 colony size phenotype as well as the ability to grow in non-fermentable carbon
258 sources (Gly⁻ phenotype).

259 No significant differences were found in the percentage of petite colonies
260 between the strains; however, a higher proportion was observed in BG14 after
261 exposure to NØ. A higher percentage of petite colonies was observed in the BG14
262 strain compared with the no-treatment conditions. These petite colonies were
263 obtained from Gly⁺ colonies after one passage through NØ stress (Table 1).

264 Gly⁻ phenotype cells are obtained under stress conditions due to neutrophil
265 phagocytosis.

266 **The growth rate of evolved strains in CAA**

267 Since we found Gly⁻ cells that grow more slowly than Gly⁺ cells, we decided to
268 determine the growth rate of cells obtained after treatment with either NØ or RPMI,
269 compared to the BG14 that had undergone no treatment and of the Gly⁺ cells,
270 obtained after the survival assay in CAA (Table 2).

271 Cell growth was monitored for 2000 minutes at OD₆₀₀ measured every 15 min in
272 a Bioscreen apparatus. The doubling times were determined using the formula
273 **$dT = \ln_2 / (\ln OD_2 - \ln OD_1) / (t_2 - t_1)$.**

274 As shown in Table 2, the doubling time was shorter for the parental strain cells
275 with no treatment (72.88 min) compared to cells that underwent either 3 passes with
276 NØ (84.04 min $p = 0.0088$) or 3 passes in RPMI medium (85.06 min $p = 0.0047$). Gly⁻
277 strain displays longer duplication time (89.33 min $p = 0.0022$ compared to BG14).

CONDITION	DOUBLING TIME	STANDAR DESVIATION
No treatment	72.88 ^a	0.9673
NØ	84.04 ^{a-b} **	3.8436
RPMI	85.06 ^{a-c} **	3.6808
Gly- Control	89.33 ^{a-d} **	0.2291

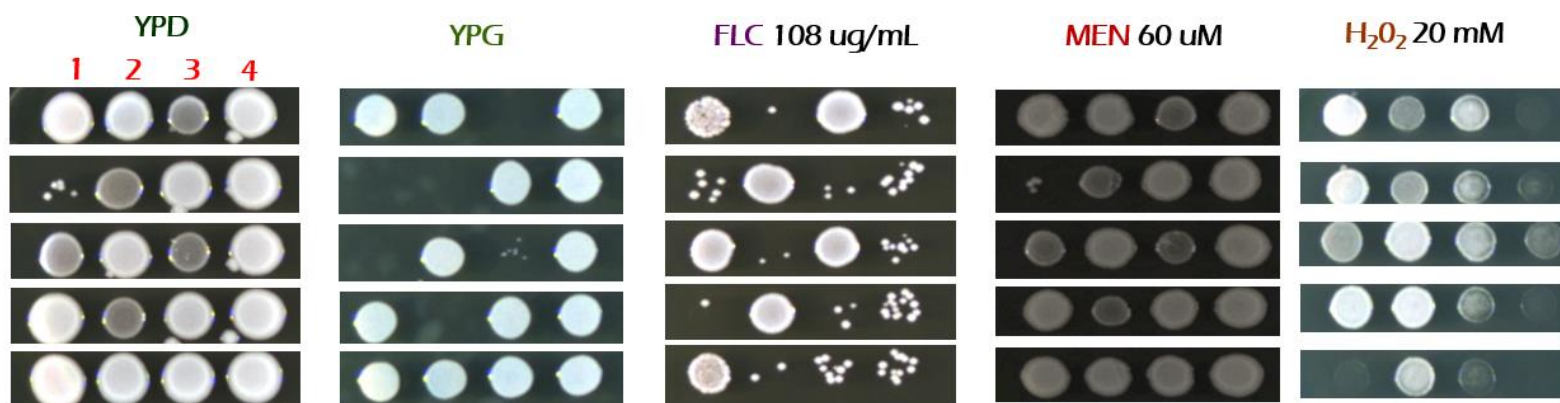
279 **Table 4| Growth curve in the synthetic complete medium of BG14 under different treatments**

280 All strains, except for Gly- is CGM1938-petite control strain generated by ethidium bromide-
 281 represents a mix of populations. The difference between groups was assessed by ANOVA test for
 282 parametric following by Tukey's multiple comparisons tests. P values ≤ 0.05 were considered
 283 statistically significant and are highlighted in bold ($*p < 0.05$, $**p < 0.01$, $***p < 0.001$). Data represents
 284 the mean of 3 technical replicates, n=1. ^a: No treatment, ^b: NØ, ^c: RPMI and ^d: Gly- control.

285 **Three consecutive passes through NØ may decrease chronic H₂O₂ exposure**
286 **of *N. glabratus*.**

287 To continue phenotypically characterizing the surviving *N. glabratus* cells, we
288 determined the response of the cells that had been exposed to NØ or RPMI for 3
289 consecutive passes to different types of oxidative stress, and antifungals (FLC) (Fig.
290 2).

291 Cells were grown up to stationary phase in 5 mL of YPD medium two ON at 30°C
292 with shaking, the OD was measured (OD₆₀₀) and set at 0.5. Each sample was spotted
293 7 µL on different indicated plates made by spot assay and incubated for 48 hours at
294 30°C.



	1	2	3	4
BG14		Gr NØ	Ch INPUT	NØ R2
CGM1938		Ch RPMI	Gr INPUT	NØ R3
Ch NØ		Gr RPMI	Ch INPUT	RPMI R1
Gr NØ		Ch RPMI	Gr INPUT	RPMI R2
Ch NØ		Gr RPMI	NØ R1	RPMI R3

295 **Fig. 2| Spot assay under different oxidative stress types and fluconazole.** Abbreviations Ch: Gly-
 296 phenotype colonies, Gr: Gly⁺ phenotype colonies, FLC: fluconazole, MEN: menadione, H₂O₂:
 297 hydrogen peroxide, INPUT: colonies without stress conditions, Rn: technical replicate. Strain
 298 CGM1938 is a Gly⁻ strain derived from treatment of BG14 with ethidium bromide. The differences
 299 between columns 1 and 2 versus 4 is the number of passes: columns 1 and 2 have 3 passes through
 300 NØ plus a survival assay and column 4 has three passes through NØ.

301

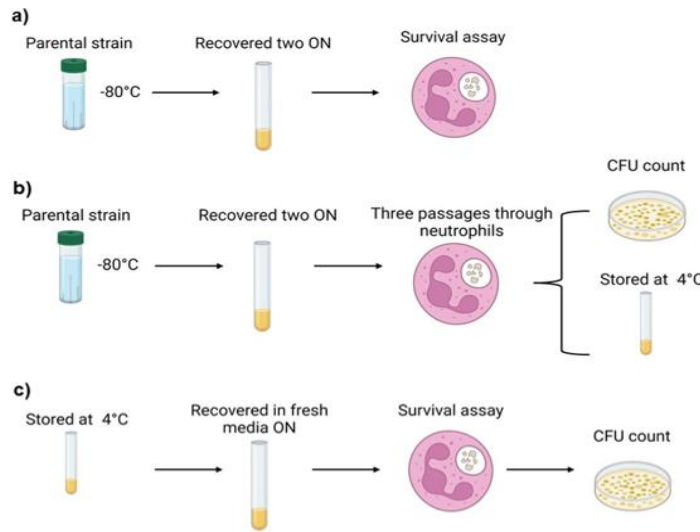
302 Notably, petite cells (obtained by exposure to NØ and RPMI medium) show
 303 greater resistance to FLC compared to Gly⁺ cells exposed to RPMI or NØ; this result
 304 was expected from previous reports describing that petite colonies have higher
 305 resistance to FLC. On the other hand, no differences were observed in the different
 306 oxidative stress conditions compared to the parental strain (BG14) and the
 307 CGM1938 (petite control strain created by ethidium bromide). However, greater
 308 sensitivity to hydrogen peroxide is observed in the spots from column four (three
 309 passes through NØ) compared to columns one and two (three passes through NØ
 310 plus a survival assay total of eight passes).

311 **Microevolution in *N. glabratus* clinical isolates.**

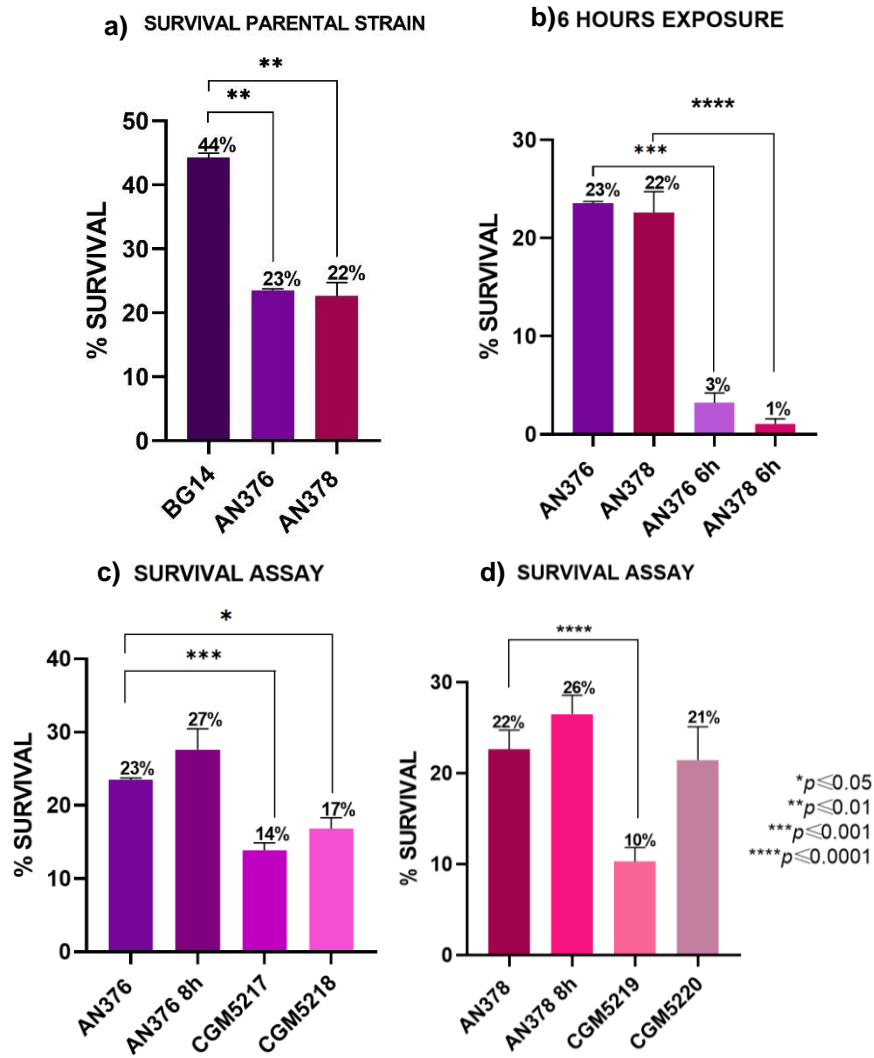
312 To test whether there are differences in the response (and adaptation and/or
313 microevolution) to NØ between *N. glabratus* strains, we decided to start the
314 characterization of clinical isolates AN376 and AN378 because these are strains
315 unrelated to our standard laboratory strain BG14 and are isolates obtained from a
316 single patient but differ in their antifungal susceptibility phenotype (Fig. 3).

317 Cells were exposed to NØ and RPMI medium for three 2-hour passages.
318 Subsequently, cells were stored at 4°C. The cells were inoculated into YPD and
319 incubated for one ON and a survival assay was performed again at 37°C with 5%
320 CO₂ for two hours (Fig. 3).

321



322



323

324

325

Fig. 3| Survival assay in *N. glabratus* clinical isolates after 3 (2-hour) passages through NØ. a) Parental strains, exposure to NØ for two h (survival assay) n=3, b) Percent survival after 6 h exposure

326 to NØ n=1 (three passes through NØ) AN376: % survival of parental strain; AN378: % survival of
327 parental strain; AN376 6h: three consecutive passages of two h each through NØ, six h in total;
328 AN378 6h: three consecutive passages of two h each through NØ, six h in total. c) Survival assay of
329 strains recovered after the 6 h exposure to NØ (eight hours total exposure): AN376: % survival of
330 parental strain; AN376 8h: three consecutive passages of two h each through NØ, plus one survival
331 assay, eight h in total; CGM5217 and CGM5218: colonies derived from AN376 with eight h exposure
332 in total n=3. d) AN378: % survival of parental strain; AN378 8h: three consecutive passages of two h
333 each through NØ, plus one survival assay, eight h in total; CGM5219 and CGM5220 colonies derived
334 from AN378 with eight h exposure in total n=3. Difference between groups was assessed by Ordinary
335 one-way ANOVA followed by Tukey's multiple comparisons post-hoc test according to data normality.
336 P-values ≤ 0.05 were considered statistically significant.

337
338 After three passages through NØ cells, the clinical isolates AN376 and AN378
339 showed significantly lower survival rates (3% and 1% respectively) compared to the
340 reference strain (44%). By comparison, the parental strains display much higher
341 survival rates (AN376: 23%, $p = <0.0001$, AN378: 22%, $p = <0.0001$) (Fig. 3a and
342 3b). Interestingly, the population of survivors from the 3 passages through NØ (cells
343 recovered from the survival assay shown in Fig. 3b), have a similar survival rate to
344 that of their respective parental strains. Therefore, we did not see a higher acquired
345 survival rate after the microevolution experiment (AN376: 23% compared to 27%
346 after the microevolution experiment, and AN378: 22% vs 26%, survival after the
347 three consecutive passages through NØ). (AN376: $p = 0.2162$, AN378: $p = 0.2813$).

348 We decided to isolate individual colonies of AN376 and AN378 strains after
349 successive passages through NØ. Colony CGM5217 exhibited a small colony
350 phenotype, while CGM5218 displayed a regular colony size originated from the
351 AN376 isolate. Similarly, colony CGM5219 exhibited a regular colony size
352 phenotype, while CGM5220 had a small size; these colonies were derived from
353 AN378. These colonies, once isolated and purified, underwent a survival assay, and
354 the resulting percentages were compared with those of their parental strains and the
355 8-hour population exposed to NØ. In contrast to the survival rate of the AN376
356 parental strain (AN376: 23%), isolated colonies derived from this strain exhibit a
357 reduced survival rate (CGM5217: 14%, $p = 0.0004$ and CGM5218: 17%, $p = 0.0178$,
358 respectively), additionally, both CGM5217 and CGM5218 show significantly smaller

359 survival rates (CGM5217: $p = < 0.0001$ and CGM5218: $p = 0.0001$) compared to
360 the AN376 mixed evolved population (AN376 8h: 27% see Fig. 3c).

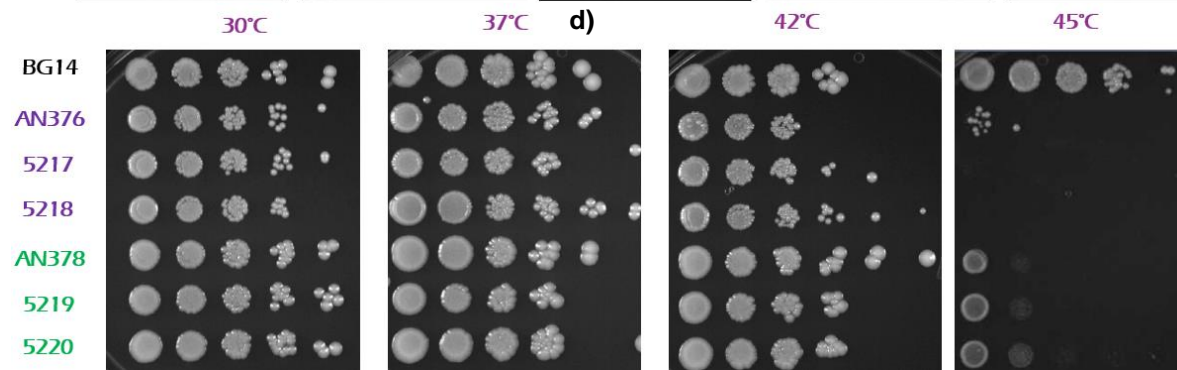
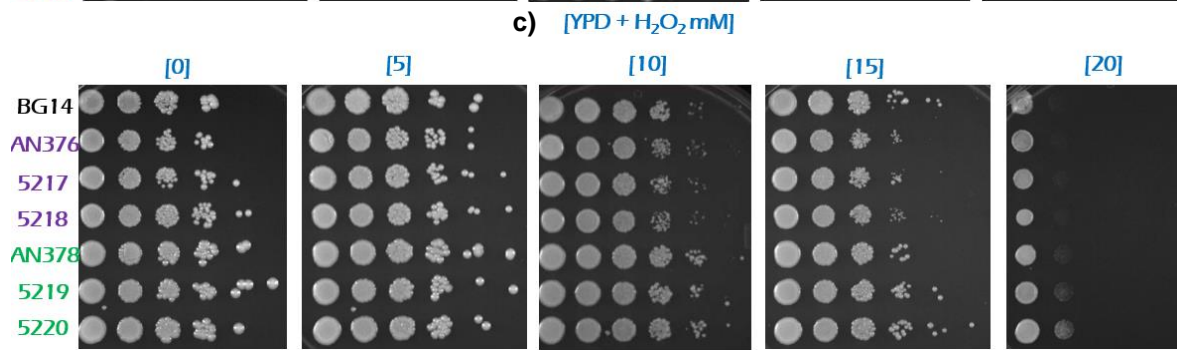
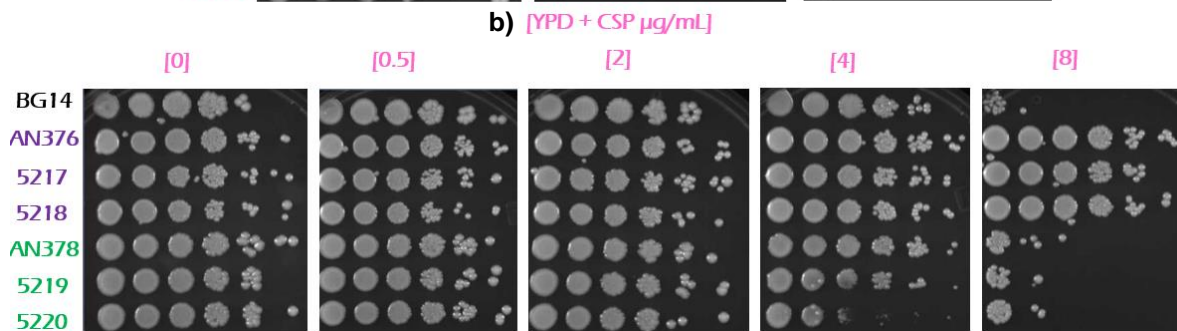
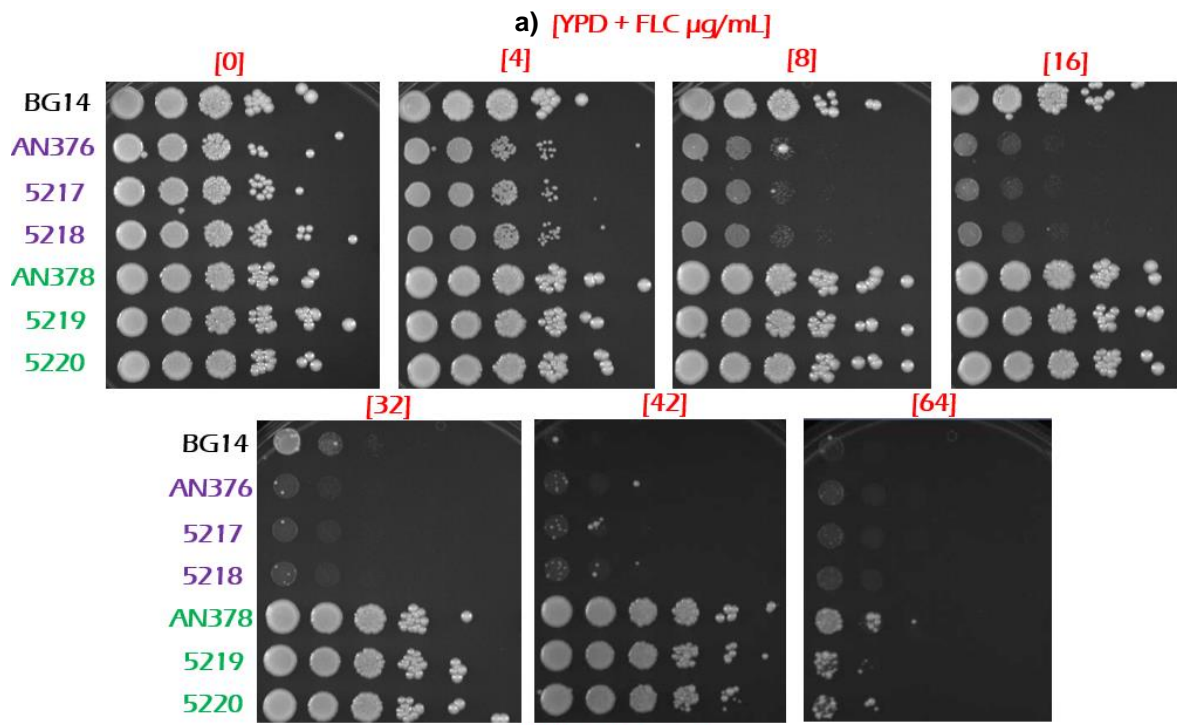
361 Upon comparing the survival percentages of colonies derived from AN378 (Fig.
362 3d), significant differences were noted between colonies CGM5219 and CGM5220
363 ($p = 0.0002$). Furthermore, it is evident that the isolated colony CGM5219 exhibits
364 lower survival compared to both its parent (CGM5219: 10%, $p = < 0.0001$) and the
365 AN378 population (AN378 8h: 26%, $p = < 0.0001$). Conversely, the survival rate of
366 colony CGM5220 remains similar to that of its parent (CGM5220: 21%, $p = 0.9995$).

367 Consecutive passes through NØ do not confer greater resistance in either of the
368 clinical isolates.

369

370 **Phenotypic characterization of the surviving *N. glabratus* clinical isolates.**

371 We decided to continue phenotypically characterizing the surviving *N. glabratus*
372 cells: we determined the response H₂O₂, antifungals (FLC and CSP), and
373 temperature stress of the cells that had been exposed to NØ for 3 consecutive
374 passes (Fig. 4)



379 **Fig. 4| Spot assay under different oxidative stress types and fluconazole of the *N. glabratus***
380 **clinical isolates.** Abbreviations FLC: fluconazole, CSP: caspofungin, H₂O₂: hydrogen peroxide,
381 BG14: reference strain. AN376: clinical isolates strain, CGM5217: isolated colony of AN376 strain
382 after six h of exposure to NØ with small colony phenotype, CGM5218: regular colony size originated
383 from the AN376 after six h to NØ, CGM5219: isolated colony of AN378 strain after six h of exposure
384 to NØ with regular colony phenotype, CGM5220: small colony size originated from the AN378 after
385 six h to NØ. n=3

386
387 Following neutrophil passages, we isolated and purified colonies from isolate
388 AN376 (CGM5217 and CGM5218) and AN378 (CGM5219 and CGM5220),
389 respectively. These colonies underwent various stress tests, and the results were
390 compared to their parental strains (retrieved from the glycerol stock) and the
391 reference strain BG14.

392 As depicted in Fig. 4a, no differences in susceptibility/resistance to FLC were
393 observed compared to their parental strains. As we had previously determined in the
394 laboratory, isolate AN376 exhibited heightened susceptibility to FLC compared to
395 BG14 and the evolved derivatives, CGM5217 and CGM5218 colonies showed the
396 same susceptibility.

397 To explore potential alterations in resistance/susceptibility to a different class of
398 antifungals such as CSP (Fig. 4b), which targets the 1-3 β -glucan synthase essential
399 for maintaining *N. glabratus*' cell wall integrity, resistance to CSP was observed in
400 isolate AN376, and its evolved derivatives colonies CGM5217 and CGM5218 [8
401 $\mu\text{g}/\text{mL}$] compared to BG14 and AN378. Interestingly, the isolated colony CGM5220,
402 which evolved from AN378, displayed increased sensitivity to CSP [4 $\mu\text{g}/\text{mL}$]
403 compared to its parent strain.

404 In addition, we did not find discernible differences between the strains when
405 compared to each other regarding their response to oxidant stress, H₂O₂ (Fig. 4c),
406 nor to heat shock (Fig. 4d).

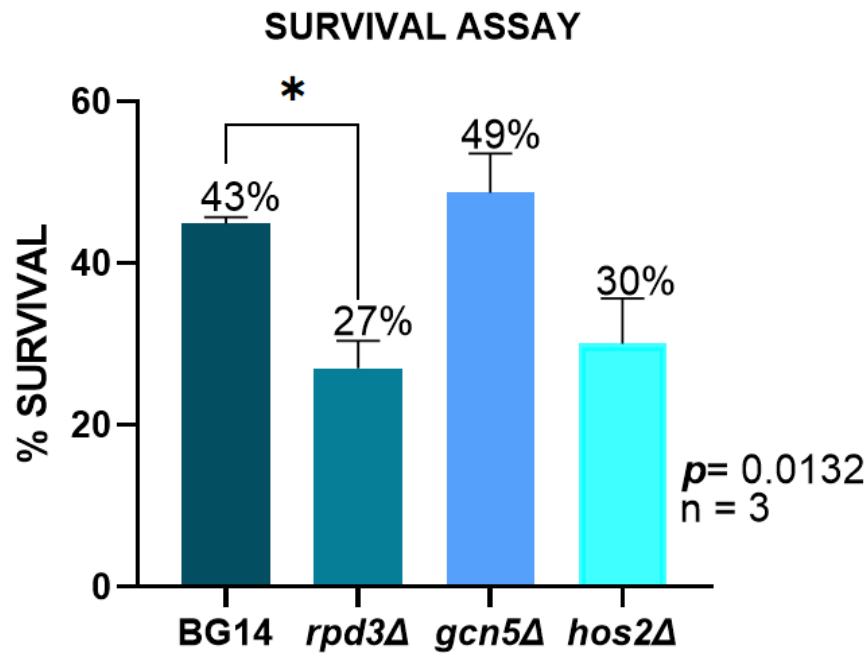
407 Although AN376 and its respective derivatives are temperature sensitive at 45°C
408 while AN378 is not as sensitive compared to BG14.

409 Therefore, serial passages through NØ did not confer greater resistance to FLC
410 or H₂O₂ exposure. Nevertheless, colony CGM5220 exhibited sensitivity to CSP
411 compared to AN378.

412

413 ***N. glabratus* mutants in histone deacetylases are involved in survival to NØ**
414 **attack.**

415 We next asked whether epigenetic mechanisms, particularly histone acetylation,
416 participate in the response to NØ. To do this, we generated knockout mutants by
417 fusion PCR in the BG14 strain genetic background in *GCN5* (*gnc5Δ*) encoding the
418 histone deacetylase (HAT) Gcn5, and in the genes *RPD3* and *HOS2* (*rpd3Δ* and
419 *hos2Δ*) encoding two histone deacetylases (HDAC). We then measured the survival
420 to NØ of these mutants (Fig. 5).



421

422 Fig. 5| Survival assay in *N. glabratus* knockout mutants after 2-hour passages through NØ. The
 423 difference between groups was assessed by Ordinary one-way ANOVA followed by Turkey's multiple
 424 comparisons post-hoc test according to data normality (* $p < 0.05$). P-values ≤ 0.05 were considered
 425 statistically significant $n=3$.

426

427 After the survival assay (a single passage through NØ), it is evident that the
 428 survival percentage of the *rpd3Δ* strain is lower than that of BG14 (*rpd3Δ*: 43%, $p =$
 429 0.0367 vs BG14: 43%). Although not statistically significant, a trend toward lower
 430 survival is also observed in the *hos2Δ* strain (*hos2Δ*: 30%, $p = 0.0801$). Conversely,
 431 the *gcn5Δ* mutant exhibited no significant differences in survival percentage
 432 compared to the reference strain (*gcn5Δ*: 49%, $p = 0.8470$).

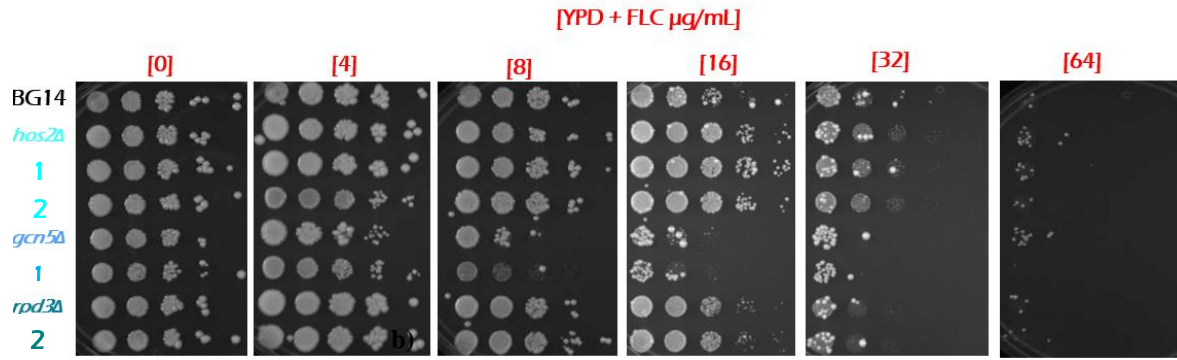
433 To continue phenotypically characterizing the surviving *N. glabratus* knockout
 434 mutants: we determined the response H₂O₂, antifungals (FLC and CSP) and
 435 temperature stress of the histone acetylation/deacetylation mutant strains and the
 436 derived colonies that had been exposed to NØ.

437 **Phenotypic characterization of the surviving *N. glabratus* knockout mutants.**

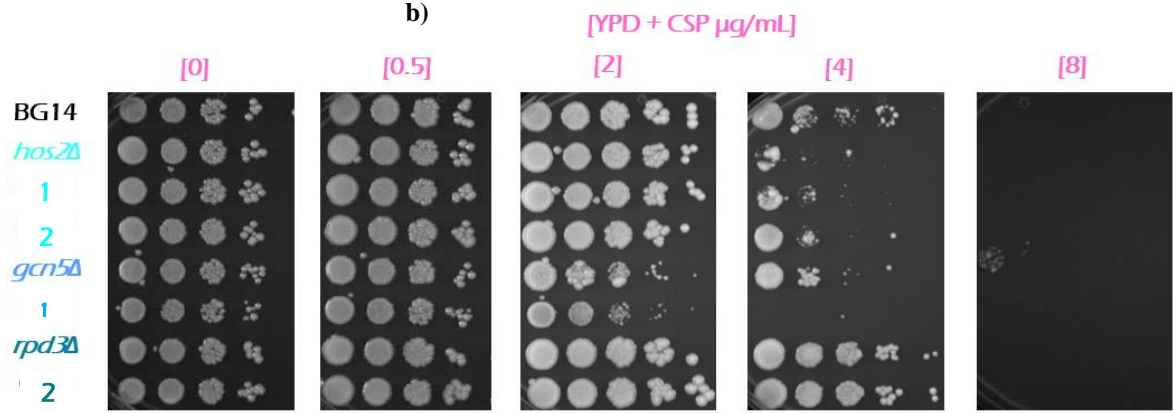
438 To continue phenotypically characterizing the surviving *N. glabratus* knockout
439 mutants, we determined the response H₂O₂, antifungals (FLC and CSP) and
440 temperature stress of the histone acetylation/deacetylation mutant strains and the
441 derived colonies that had been exposed to NØ (Fig. 6).

442

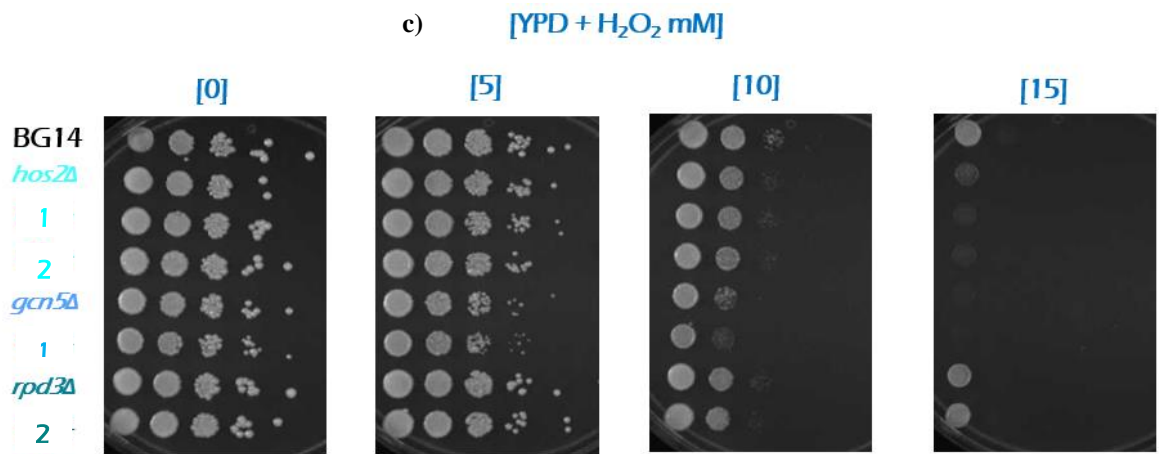
a)

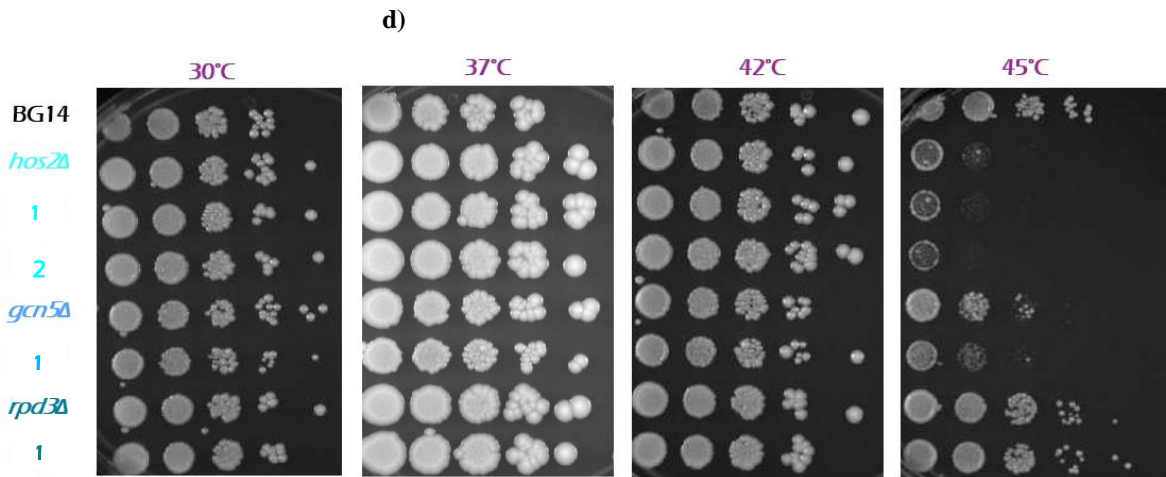


b)



c)





446

447 **Fig. 6| Spot assay under different oxidative stress conditions and fluconazole of the histone**
 448 **acetylation/deacetylation knockout mutants.** Abbreviations FLC: fluconazole, CSP: caspofungin,
 449 H₂O₂: hydrogen peroxide, BG14: reference strain. *hos2Δ*: recovered strain, 1: regular size colony
 450 isolated of *hos2Δ* strain after two h of exposure to NØ, 2: regular colony size originated from *hos2Δ*
 451 after two h to NØ, *gcn5Δ*: recovered glycerol strain, 1: regular size colony isolated of *gcn5Δ* strain
 452 after two h of exposure to NØ, *rpd3Δ*: recovered glycerol strain, 1: regular size colony isolated of
 453 *rpd3Δ* strain after two h of exposure to NØ. n=2

454

455 After the NØ assay, we isolated and purified colonies obtained from *hos2Δ*
 456 (colonies 1 and 2), *gcn5Δ* (1) and *rpd3Δ* (1) respectively and we tested these
 457 colonies onto various stress tests compared to their parental strains and BG14
 458 strain.

459 The results of chronic stress exposure to FLC are shown in Fig. 6a. FLC
 460 sensitivity is evident in the parental strain *gcn5Δ* and its derived colony [16 µg/mL]
 461 compared to BG14. We did not find significant differences in resistance to FLC at 32
 462 µg/mL observed in the *hos2Δ*.

463 Regarding the resistance/susceptibility phenotypes to CSP (Fig. 6b), no
 464 differences were observed between *rpd3Δ* and BG14. In contrast, *hos2Δ* and its
 465 derivatives exhibited increased sensitivity at 4 µg/mL compared to the WT.
 466 Additionally, the colony derived from *gcn5Δ* after NØ exposure demonstrated
 467 significantly greater resistance to CPS [2 µg/mL] compared to its parent and the
 468 reference strain. On the other hand, no differences were noted in growth phenotypes
 469 when exposed to H₂O₂ (Fig. 6c) versus BG14 strain.

470 Furthermore, when evaluating the response to temperature stress (Fig. 6d), a
 471 sensitivity phenotype was observed at 45°C in *hos2Δ* and colonies derived from it

472 and in the *gcn5Δ* two h exposure colony derived from the *gcn5Δ* parental strain,
473 compared to BG14. No differences in the temperature stress response were
474 observed in the *rdp3Δ* mutant compared to the parent strain.

475

Discussion

476 **Consecutive passages through NØ do not enhance resistance to NØ.**

477 Recently some investigations have studied the microevolution of *N. glabratus*
478 during the infection of human hosts and the development of antifungal resistance
479 (Badrane et al., 2023; López-Marmolejo et al., 2024). However, it remains unclear
480 whether *N. glabratus* cells exhibit microevolution *in vitro* when exposed to cells of
481 the innate immune system. Innate immunity plays a crucial role in combating and
482 preventing infections caused by opportunistic fungi. Phagocytic cells, such as NØ,
483 act as the first line of defense by recognizing these pathogenic fungi (Salgado et al.,
484 2021). *N. glabratus* relies on inducing a low-grade inflammatory response and silent
485 transit within the host, delaying neutrophil activation (Shantal et al., 2022). However,
486 the mechanisms by which *N. glabratus* evades neutrophil activity have not been
487 extensively studied.

488 In this study, for the first time, we evaluated *in vitro* microevolution of clinical
489 isolates and a reference strain of *N. glabratus*. Through three passages to induce
490 microevolution, we observed a slight increase in the survival trends of Gly⁺ cells.
491 Nonetheless, no significant difference was noted in the survival rate of the Gly⁻
492 phenotype compared to untreated cells (Fig. 1). In clinical isolates AN376 and
493 AN378, three consecutive passages through NØ (evolved cells) resulted in
494 significant loss of viability as measured by a survival assay of the recovered cells
495 (Fig. 2b). However, the isolated evolved survivors of the three passages through NØ
496 (cells recovered from the survival assay shown in Fig. 2b), retained a similar survival
497 rate to their respective parental strain (evolved from AN736: 22%, compared to the
498 parental AN376 27%, and parental strain AN378: 22% compared to evolved AN378:
499 26%; Fig. 2c). Therefore, we do not observe any microevolution that enables it to
500 better survive increased levels to NØ.

501 Although we did not observe enhanced resistance to NØ as a result of
502 microevolution, Badrane et al., 2023 have reported *N. glabratus* clinical isolates
503 resistant to phagocytosis and death by NØ. Overall, passages through NØ do not
504 confer greater resistance in clinical isolates or the laboratory reference strain BG14.
505 Further research is needed to elucidate these mechanisms, which are essential for
506 developing drugs targeting these adaptations.

507 ***N. glabratus* mutants *rpd3Δ* and *hos2Δ* are involved in the survival against**
508 **NØ.**

509 In this study, we present novel findings demonstrating the involvement of HDACs
510 (*CgRpd3* and *CgHos2*) in *N. glabratus* survival under NØ stress (Fig. 5), as well as
511 their response to thermal stress (Fig. 6). Rpd3 and Hos2 belong to the same family
512 of class I histone deacetylases in *S. cerevisiae* (Kurdistani and Grunstein, 2003).
513 *ScRpd3* and *ScHos2* show some redundancy in the genes they regulate like, *RNR3*
514 and *HUG1* genes, and elimination of these HDACs leads to hyper-acetylation to
515 different degrees, in several common genes like: *ERG11*, *GAL7*, *GAL10*, and *GAL1*.
516 Rpd3 is required for deacetylation of H3, H2B and H4 except for H4K16, and Hos2
517 for deacetylation of H4-K16 (Kurdistani and Grunstein, 2003; Sharma et al., 2007;
518 Wang et al., 2002). Rpd3 activity is associated with the activation of osmotic stress
519 response gene expression in *S. cerevisiae*, as well as in azole resistance in *C.*
520 *albicans*, while Hos2 is necessary for chromatin deacetylation and recruitment to the
521 open reading frames (ORFs) of different genes (De Nadal et al., 2004; Li et al., 2015;
522 Sharma et al., 2007). Our study reveals that the survival percentage of these
523 knockout mutants is lower than that of the parental strain BG14 (*rpd3Δ*: 27%, *hos2Δ*:
524 30% compared to 41% in the parental BG14).

525 Previous studies have reported the involvement of *ScHos2* and *ScRpd3* in
526 regulating the transcriptional activation of DNA damage response genes, directly
527 positively regulating *RNR3* and *HUG1* (Sharma et al., 2007). Fukuda et al., 2013
528 evaluated the transcriptional profile of *N. glabratus* during phagocytosis by NØ and
529 found that 5% of the 339 upregulated genes corresponded to DNA repair processes.
530 Based on this information, we propose that the lower survival percentage observed
531 in our study may be due to the inefficient transcriptional activation of DNA damage

532 response genes resulting from HDACs elimination. Consequently, the production of
533 ROS from NØ may cause DNA damage that is not adequately repaired. However,
534 further investigation is required to confirm these findings by quantifying ROS
535 production by NØ.

536 Filler et al., 2021 identified that Rpd3 is necessary for *N. glabratus* for virulence,
537 as the mutant exhibited attenuated virulence in a neutropenic mice model.
538 Additionally, susceptibility assays to host defense peptides revealed that the
539 CgRpd3 mutant showed susceptibility to human neutrophil peptide-1 (hNP-1),
540 whereas Cghos2Δ strain displayed a response similar to its parent strain (CBS138
541 strain) to hNP-1 but sensitivity to protamine, an antimicrobial compound. We
542 demonstrate the involvement of HDACs in NØ survival mechanisms, possibly
543 induced by defects in DNA repair caused by NØ-derived ROS. However,
544 confirmation of these findings awaits further investigation into ROS production by
545 NØ and DNA repair mechanisms in the mutants.

546 **Gcn5 is not involved in the survival to NØ.**

547 GCN5 is part of the SAGA complex with histone acetyltransferase (HAT) activity.
548 Previous studies have reported the role of CgGcn5 in modulating virulence and
549 regulating replication within macrophages in *N. glabratus* (Yu et al., 2022), although
550 there are no reported data on NØ survival. Our findings indicate that exposing the
551 *gcn5Δ* mutant to NØ did not alter the survival percentage compared to its parent
552 strain, suggesting that Gcn5 may not be involved in NØ resistance, unlike the
553 responses to macrophages where the *gcn5Δ* mutant is more sensitive than the
554 parental strain.

555 **The epigenetic response participates in different types of stress.**

556 Previous studies have evaluated the involvement of the epigenetic response in
557 antifungal resistance mechanisms. In this study, we assessed the response to FLC,
558 CSP, H₂O₂, and temperature, in mutants generated in BG14 background and,
559 colonies derived after NØ confrontation (Fig. 6).

560 Pfaller et al., 2009 evaluated the synergistic effect of a drug inhibiting CgHos2
561 activity (MGCD290) combined with three different azoles (FLC, posaconazole, and

562 voriconazole). They observed increased sensitivity in clinical isolates of *N. glabratus*
563 previously reported as resistant when treated with this combination. On the other
564 hand, Yu et al., 2022 reported that eliminating *GCN5* increased the sensitivity to FLC
565 in the CBS138 strain. These results align with the findings found in this study, where
566 a slight sensitivity to 4 µg/mL was observed in the *gcn5Δ* and *hos2Δ* compared to
567 the WT. Interestingly, the *rpd3* mutant did not exhibit any phenotypic change. Thus,
568 we confirmed the role of these histone modifiers in resistance to FLC. By observing
569 a phenotype of increased sensitivity in the colony isolated from *gcn5Δ*, we
570 demonstrated that exposure to NØ resulted in greater sensitivity to FLC. However,
571 the potential mechanisms underlying this phenotype remain to be studied.

572 Deleting *rpd3*, *hos2* and *gcn5* in *N. glabratus* CBS138 background increases
573 susceptibility to CSP and Micafungin (Filler et al., 2021; Schwarzmüller et al., 2014;
574 Yu et al., 2022). Additionally, a synergistic effect has been observed in clinical
575 isolates of *N. glabratus*, showing a 46.7-53.3% increase in sensitivity when treated
576 with MGCD290+CSP, and reversing resistance in isolates with FKS mutations
577 (Pfaller et al., 2015). When we evaluated the response to CSP
578 susceptibility/resistance (Fig. 6b), we observed differences in growth among *gcn5Δ*
579 with BG14 strain. These data are consistent with susceptibility to CSP in the *gcn5Δ*
580 background but not *rpd3Δ*. Interestingly, *hos2Δ* exhibited a slightly increased
581 sensitivity to CPS compared to the WT strain. The results suggest that Hos2 and
582 Gcn5 play an important role in CPS resistance. The resistance to CPS observed in
583 Gcn5 may be attributed to its role in regulating the FKS genes (Yu et al., 2022),
584 which are essential for maintaining the cell wall of *N. glabratus*. However, the
585 mechanisms utilized by Hos2 remain to be studied.

586 When testing H₂O₂ sensitivity, we observed a modest increase in susceptibility in
587 *gcn5* mutant and its derived colony, but not in other strains (Fig. 6c). This confirms
588 previous reports that CgGcn5 is related to resistance to this type of stress (Filler et
589 al., 2021). Deleting this gene in *N. glabratus* increases sensitivity to H₂O₂ (10mM)
590 compared to CBS138 standard strain (Lin et al., 2023; Yu et al., 2022). However,
591 resistance to H₂O₂ is not affected by mutations in *rpd3Δ* or *hos2Δ* in our study and
592 Filler et al., 2021, suggesting that HAT (*Gcn5*) is responsible for H₂O₂ resistance,
593 while HDACs do not play a significant role.

594 Finally, we evaluated the response to temperature stress. ScRpd3 has been
595 proposed to fine-tune the transcriptional response under temperature shock (Kremer
596 and Gross, 2009). There is no other reference in the literature, and further studies
597 are needed to address this question. We evaluated the involvement of the epigenetic
598 response in resistance to temperature shock in *N. glabratus* (Fig. 6d). For the first
599 time, we described that mutants and colonies derived from *hos2Δ* and *gcn5Δ* are
600 more sensitive to growth at 45°C compared to the control. Therefore, we propose
601 that Gcn5 and Hos2 are involved in the heat shock response in *N. glabratus*.

602 In conclusion, our findings show that three passes through NØ do not increase
603 the resistance to NØ in the *N. glabratus* clinical isolates and BG14 strain. We
604 demonstrated for the first time that Rpd3 and Hos2 are involved in the survival of
605 *N. glabratus* to NØ, whereas Gcn5 is not. This discovery could pave the way for
606 identifying new targets for drug development.

References

- 607
608 De Las Peñas, Alejandro, Jacqueline Juárez-Cepeda, Eunice López-Fuentes,
609 Marcela. Briones-Martín-del-Campo, Guadalupe Gutiérrez-Escobedo, and
610 Irene Castaño. "Local and Regional Chromatin Silencing in *Candida Glabrata*:
611 Consequences for Adhesion and the Response to Stress." Edited by Monique
612 Bolotin-Fukuhara. *FEMS Yeast Research* 15, no. 6 (September 2015):
613 fov056. <https://doi.org/10.1093/femsyr/fov056>.
- 614 Badrane, H., Cheng, S., Dupont, C., Hao, B., Driscoll, E., Morder, K., Liu, G.,
615 Newbrough, A., Fleres, G., Kaul, D., Espinoza, J., Clancy, C., Nguyen, M.H.,
616 2023. Genotypic diversity and unrecognized antifungal resistance among
617 populations of *Candida glabrata* from positive blood cultures.
618 <https://doi.org/10.21203/rs.3.rs-2706400/v1>
- 619 Castaño, I., Kaur, R., Pan, S., Cregg, R., Peñas, A.D.L., Guo, N., Biery, M.C., Craig,
620 N.L., Cormack, B.P., 2003. Tn 7 -Based Genome-Wide Random Insertional
621 Mutagenesis of *Candida glabrata*. *Genome Res.* 13, 905–915.
622 <https://doi.org/10.1101/gr.848203>
- 623 De Nadal, E., Zapater, M., Alepuz, P.M., Sumoy, L., Mas, G., Posas, F., 2004. The
624 MAPK Hog1 recruits Rpd3 histone deacetylase to activate osmoresponsive
625 genes. *Nature* 427, 370–374. <https://doi.org/10.1038/nature02258>
- 626 Ermert, D., Zychlinsky, A., Urban, C., 2009. Fungal and Bacterial Killing by
627 Neutrophils, in: Rupp, S., Sohn, K. (Eds.), *Host-Pathogen Interactions*,
628 *Methods in Molecular Biology*. Humana Press, Totowa, NJ, pp. 293–312.
629 https://doi.org/10.1007/978-1-59745-204-5_21
- 630 Essig, F., Hünninger, K., Dietrich, S., Figge, M.T., Kurzai, O., 2015. Human
631 neutrophils dump *Candida glabrata* after intracellular killing. *Fungal Genetics*
632 *and Biology* 84, 37–40. <https://doi.org/10.1016/j.fgb.2015.09.008>
- 633 Filler, E.E., Liu, Y., Solis, N.V., Wang, L., Diaz, L.F., Edwards, J.E., Filler, S.G.,
634 Yeaman, M.R., 2021a. Identification of *Candida glabrata* Transcriptional
635 Regulators That Govern Stress Resistance and Virulence. *Infect Immun* 89,
636 e00146-20. <https://doi.org/10.1128/IAI.00146-20>
- 637 Filler, E.E., Liu, Y., Solis, N.V., Wang, L., Diaz, L.F., Edwards, J.E., Filler, S.G.,
638 Yeaman, M.R., 2021b. Identification of *Candida glabrata* Transcriptional

639 Regulators That Govern Stress Resistance and Virulence. *Infect Immun* 89,
640 e00146-20. <https://doi.org/10.1128/IAI.00146-20>

641 Fukuda, Y., Tsai, H.-F., Myers, T.G., Bennett, J.E., 2013. Transcriptional Profiling of
642 *Candida glabrata* during Phagocytosis by Neutrophils and in the Infected
643 Mouse Spleen. *Infect Immun* 81, 1325–1333.
644 <https://doi.org/10.1128/IAI.00851-12>

645 Gutiérrez-Escobedo, G., Hernández-Carreón, O., Morales-Rojano, B., Revuelta-
646 Rodríguez, B., Vázquez-Franco, N., Castaño, I., De Las Peñas, A., 2020.
647 *Candida glabrata* peroxiredoxins, Tsa1 and Tsa2, and sulfiredoxin, Srx1,
648 protect against oxidative damage and are necessary for virulence. *Fungal*
649 *Genetics and Biology* 135, 103287. <https://doi.org/10.1016/j.fgb.2019.103287>

650 Gutiérrez-Escobedo, G., Vázquez-Franco, N., López-Marmolejo, A., Luna-Arvizu,
651 G., Cañas-Villamar, I., Castaño, I., De Las Peñas, A., 2023. Characterization
652 of the Trr/Trx system in the fungal pathogen *Candida glabrata*. *Fungal*
653 *Genetics and Biology* 166, 103799. <https://doi.org/10.1016/j.fgb.2023.103799>

654 Kremer, S.B., Gross, D.S., 2009. SAGA and Rpd3 Chromatin Modification
655 Complexes Dynamically Regulate Heat Shock Gene Structure and
656 Expression. *Journal of Biological Chemistry* 284, 32914–32931.
657 <https://doi.org/10.1074/jbc.M109.058610>

658 Kurdistani, S.K., Grunstein, M., 2003. Histone acetylation and deacetylation in yeast.
659 *Nat Rev Mol Cell Biol* 4, 276–284. <https://doi.org/10.1038/nrm1075>

660 Li, X., Cai, Q., Mei, H., Zhou, X., Shen, Y., Li, D., Liu, W., 2015. The Rpd3/Hda1
661 family of histone deacetylases regulates azole resistance in *Candida*
662 *albicans*. *Journal of Antimicrobial Chemotherapy* 70, 1993–2003.
663 <https://doi.org/10.1093/jac/dkv070>

664 Lin, C.-J., Yang, S.-Y., Hsu, L.-H., Yu, S.-J., Chen, Y.-L., 2023. The Gcn5-Ada2-
665 Ada3 histone acetyltransferase module has divergent roles in pathogenesis
666 of *Candida glabrata*. *Medical Mycology* 61, myad004.
667 <https://doi.org/10.1093/mmy/myad004>

668 López-Marmolejo, A.L., Hernández-Chávez, M.J., Gutiérrez-Escobedo, G., Selene
669 Herrera-Basurto, M., Mora-Montes, H.M., De Las Peñas, A., Castaño, I.,
670 2024. Microevolution of *Candida glabrata* (*Nakaseomyces glabrata*) during

671 an infection. *Fungal Genetics and Biology* 172, 103891.
672 <https://doi.org/10.1016/j.fgb.2024.103891>

673 Pais, P., Galocha, M., Viana, R., Cavalheiro, M., Pereira, D., Teixeira, M.C., 2019.
674 Microevolution of the pathogenic yeasts *Candida albicans* and *Candida*
675 *glabrata* during antifungal therapy and host infection. *Microb Cell* 6, 142–159.
676 <https://doi.org/10.15698/mic2019.03.670>

677 Pfaller, M.A., Messer, S.A., Georgopapadaku, N., Martell, L.A., Besterman, J.M.,
678 Diekema, D.J., 2009. Activity of MGCD290, a Hos2 Histone Deacetylase
679 Inhibitor, in Combination with Azole Antifungals against Opportunistic Fungal
680 Pathogens. *J Clin Microbiol* 47, 3797–3804.
681 <https://doi.org/10.1128/JCM.00618-09>

682 Pfaller, M.A., Rhomberg, P.R., Messer, S.A., Castanheira, M., 2015. In vitro activity
683 of a Hos2 deacetylase inhibitor, MGCD290, in combination with
684 echinocandins against echinocandin-resistant *Candida* species. *Diagnostic*
685 *Microbiology and Infectious Disease* 81, 259–263.
686 <https://doi.org/10.1016/j.diagmicrobio.2014.11.008>

687 Salgado, R.C., Fonseca, D.L.M., Marques, A.H.C., Da Silva Napoleao, S.M., França,
688 T.T., Akashi, K.T., De Souza Prado, C.A., Baiocchi, G.C., Praça, D.R.,
689 Jansen-Marques, G., Filgueiras, I.S., De Vito, R., Freire, P.P., De Miranda,
690 G.C., Camara, N.O.S., Calich, V.L.G., Ochs, H.D., Schimke, L.F., Jurisica, I.,
691 Condino-Neto, A., Cabral-Marques, O., 2021. The network interplay of
692 interferon and Toll-like receptor signaling pathways in the anti-*Candida*
693 immune response. *Sci Rep* 11, 20281. [https://doi.org/10.1038/s41598-021-](https://doi.org/10.1038/s41598-021-99838-0)
694 [99838-0](https://doi.org/10.1038/s41598-021-99838-0)

695 Schwarzmüller, T., Ma, B., Hiller, E., Istel, F., Tscherner, M., Brunke, S., Ames, L.,
696 Firon, A., Green, B., Cabral, V., Marcet-Houben, M., Jacobsen, I.D., Quintin,
697 J., Seider, K., Frohner, I., Glaser, W., Jungwirth, H., Bachellier-Bassi, S.,
698 Chauvel, M., Zeidler, U., Ferrandon, D., Gabaldón, T., Hube, B., d'Enfert, C.,
699 Rupp, S., Cormack, B., Haynes, K., Kuchler, K., 2014. Systematic
700 Phenotyping of a Large-Scale *Candida glabrata* Deletion Collection Reveals
701 Novel Antifungal Tolerance Genes. *PLoS Pathog* 10, e1004211.
702 <https://doi.org/10.1371/journal.ppat.1004211>

703 Shantal, C.-J.N., Juan, C.-C., Lizbeth, B.-U.S., Carlos, H.-G.J., Estela, G.-P.B.,
704 2022. *Candida glabrata* is a successful pathogen: An artist manipulating the
705 immune response. *Microbiological Research* 260, 127038.
706 <https://doi.org/10.1016/j.micres.2022.127038>

707 Sharma, V.M., Tomar, R.S., Dempsey, A.E., Reese, J.C., 2007. Histone
708 Deacetylases RPD3 and HOS2 Regulate the Transcriptional Activation of
709 DNA Damage-Inducible Genes. *Molecular and Cellular Biology* 27, 3199–
710 3210. <https://doi.org/10.1128/MCB.02311-06>

711 Siscar-Lewin, S., Gabaldón, T., Aldejohann, A.M., Kurzai, O., Hube, B., Brunke, S.,
712 2021. Transient Mitochondria Dysfunction Confers Fungal Cross-Resistance
713 against Phagocytic Killing and Fluconazole. *mBio* 12, e01128-21.
714 <https://doi.org/10.1128/mBio.01128-21>

715 Urban, C.F., Backman, E., 2020. Eradicating, retaining, balancing, swarming,
716 shuttling and dumping: a myriad of tasks for neutrophils during fungal
717 infection. *Current Opinion in Microbiology* 58, 106–115.
718 <https://doi.org/10.1016/j.mib.2020.09.011>

719 Vázquez-Franco, N., Gutiérrez-Escobedo, G., Juárez-Reyes, A., Orta-Zavalza, E.,
720 Castaño, I., De Las Peñas, A., 2022. *Candida glabrata* Hst1-Rfm1-Sum1
721 complex evolved to control virulence-related genes. *Fungal Genetics and*
722 *Biology* 159, 103656. <https://doi.org/10.1016/j.fgb.2021.103656>

723 Wang, A., Kurdistani, S.K., Grunstein, M., 2002. Requirement of Hos2 Histone
724 Deacetylase for Gene Activity in Yeast. *Science* 298, 1412–1414.
725 <https://doi.org/10.1126/science.1077790>

726 Yu, S., Paderu, P., Lee, A., Eirekat, S., Healey, K., Chen, L., Perlin, D.S., Zhao, Y.,
727 2022. Histone Acetylation Regulator Gcn5 Mediates Drug Resistance and
728 Virulence of *Candida glabrata*. *Microbiol Spectr* 10, e00963-22.
729 <https://doi.org/10.1128/spectrum.00963-22>

730

Supplementary material

732 **Supplementary tables.**733 **Table S1| Strains generated.**

<i>C. glabrata</i> strains	Parental	Genotype	Phenotype		Reference
BG14	BG2	<i>ura3Δ::Tn903</i> G418 ^R	Ura ⁻ Gly ⁺		Cormack and Falkow 1999
Evolved strains				Treatment	
CGM5014	BG14	<i>ura3Δ::Tn903</i> G418 ^R	Ura ⁻ Gly ⁻	Evolved 3 passes NØ	This work
CGM5015	BG14	<i>ura3Δ::Tn903</i> G418 ^R	Ura ⁻ Gly ⁻	Survival assay	This work
CGM5016	BG14	<i>ura3Δ::Tn903</i> G418 ^R	Ura ⁻ Gly ⁻	Evolved 3 passes RPMI	This work
CGM5017	BG14	<i>ura3Δ::Tn903</i> G418 ^R	Ura ⁻ Gly ⁻	Evolved 3 passes NØ	This work
CGM5018	BG14	<i>ura3Δ::Tn903</i> G418 ^R	Ura ⁻ Gly ⁻	One pass to RPMI	This work
CGM5019	BG14	<i>ura3Δ::Tn903</i> G418 ^R	Ura ⁻ Gly ⁻	Evolved 3 passes RPMI	This work
CGM5020	BG14	<i>ura3Δ::Tn903</i> G418 ^R	Ura ⁻ Gly ⁻	Survival assay	This work
CGM5021	BG14	<i>ura3Δ::Tn903</i> G418 ^R	Ura ⁻ Gly ⁺	Evolved 3 passes NØ	This work
CGM5022	BG14	<i>ura3Δ::Tn903</i> G418 ^R	Ura ⁻ Gly ⁺	Survival assay	This work
CGM5023	BG14	<i>ura3Δ::Tn903</i> G418 ^R	Ura ⁻ Gly ⁺	One pass to RPMI	This work

CGM5037	BG14	<i>ura3Δ::Tn903</i> G418 ^R	Ura ⁻ Gly ⁻	Evolved 3 passes NØ	This work
CGM5038	BG14	<i>ura3Δ::Tn903</i> G418 ^R	Ura ⁻ Gly ⁻	Evolved 3 passes RPMI	This work
CGM5039	BG14	<i>ura3Δ::Tn903</i> G418 ^R	Ura ⁻ Gly ⁻	Evolved 3 passes NØ	This work
CGM5040	BG14	<i>ura3Δ::Tn903</i> G418 ^R	Ura ⁻ Gly ⁻	One pass to RPMI	This work
CGM5041	BG14	<i>ura3Δ::Tn903</i> G418 ^R	Ura ⁻ Gly ⁻	Evolved 3 passes RPMI	This work
CGMCGM52 17	AN376	Clinical isolate	Gly ⁺	Evolved 3 passes NØ	This work
CGMCGM52 18	AN376	Clinical isolate	Small, colony, Gly ⁺	Evolved 3 passes NØ	This work
CGMCGM52 19	AN378	Clinical isolate	Gly ⁺	Evolved 3 passes NØ	This work
CGMCGM52 20	AN378	Clinical isolate	Small colony, Gly ⁺	Evolved 3 passes NØ	This work
CGM5227	AN376	Clinical isolate	Gly ⁺	Evolved 3 passes RPMI	This work
CGM5228	AN378	Clinical isolate	Gly ⁺	Evolved 3 passes RPMI	This work
CGM5229	AN378	Clinical isolate	Gly ⁻	Evolved 3 passes RPMI	This work
CGM5245	AN376	Clinical isolate	Gly ⁺	Evolved 3 passes RPMI	This work
CGM5246	AN378	Clinical isolate	Gly ⁺	Evolved 3 passes RPMI	This work
CGM5247	AN376	Clinical isolate	Small colony, Gly ⁺	Evolved 3 passes RPMI	This work

CGM5248	AN378	Clinical isolate	Small colony, Gly ⁺	Evolved 3 passes RPMI	This work
CGM5249	AN376	Clinical isolate	Gly ⁻	Evolved 3 passes RPMI	This work
Mutants			Function		
CGM5242	BG14	<i>rpd3Δ::FRT-URA3-FRT</i>	Ura ⁺ Gly ⁺	Histone deacetylase activity (targets N-terminal H4K5 and H4K12).	This work
CGM5243	BG14	<i>rpd3Δ::FRT-URA3-FRT</i>	Ura ⁺ Gly ⁺	Histone deacetylase activity (targets N-terminal H4K5 and H4K12).	This work
CGM5312	BG14	<i>gcn5Δ::FRT-URA3-FRT</i>	Ura ⁺ Gly ⁺	Histone acetyltransferase activity (targets N-terminal lysine residues K11/K16 in histone H2B and K9/K14/K18/K23/K27 in histones H3).	This work
CGM5313	BG14	<i>hos2Δ::FRT-URA3-FRT</i>	Ura ⁺ Gly ⁺	Histone acetyltransferase	This work

				se activity (targets N-terminal lysine residues K11/K16 in histone H2B and K9/K14/K18/K23/K27 in histones H3).	
CGM5314	BG14	<i>hos2Δ::FRT-URA3-FRT</i>	Ura ⁺ Gly ⁺	Histone deacetylase activity (N-terminal H4-K16)	This work

734

735 Table S2| Primers

Strain	Primers	Sequence 5' -> 3'
<i>rpd3Δ</i>	RPD3at-588Fw RPD3at-4Rv RPD3at+24Fw RPD3at+522Rv RPD3at314_Fw RPD3at816_Rv DiagRPD3at-666Fw DiagRPD3at+631Rv	GAACGCCATGTATGACAACG CGAATTCAGGAACTTGATATTTTTTCC CTATCGCTGTATTAACC GGTACCACATCGTCTTTGTA AATAACCCCAACCCTCTGC GACCCAATCCCTTAACTGCC TGTCGGTGACGATTGTCCCG ACCACATTGCAACACCACGG CTTCTCTGCAGACGACACCC GCATTCTGTCAATGGCACCC
<i>gcn5Δ</i>	GCN5@-968PBFW GCN5@-917PBFW GCN5@12PBFW GCN5@+4PBFW GCN5@-76PBRV GCN5@382PBRV GCN5@+954PBRV GCN5@+808PBRV	GGGAACAGGGTCTACGTATG GGAGGTATTGCAGTAAGAGAATG GACTGTACGCACCGTGTTAG CACGGTACCACATCGTCTTTGTT GTTAGCTTAAGGTCATGG CGAATTCAGGAACTTGATATTTTTGCTC CAAAGGGAAAGCTCTAAC GACTGTTGATGTAGTACTCGATG CGCTGTGAATTCCAAGAGC CTAATCCAGCATTACGTGGTG CAAGGTGGTTACAATATTC AATAG
<i>hos2Δ</i>	HOS2@1000PBFW HOS2@-957PBFW HOS2@60PBFW HOS2@+0PBFW HOS2@-39PBRV HOS2@339PBRV HOS2@+989PBRV HOS2@+955PBRV	GTGGACTCATGATCTCAATG CCTTCCACTGTGTCGCAG GCTCTAACTATGCGCCTCG CACGGTACCACATCGTCTTTGCAGCTACAT ACTATTTACGATAATGAGAAG CGAATCGAATTCAGGAACTTGATATTTTTCGGC TTATAATCACTAGATGAACACTTC CGGACAATCATCACCAATG GTGGCTTTGATAACTTTCTG GTGAATTCCTCAACACAGCC

736

737 **Table S3| Program fusion PCR**

First part				Second part	
Buffer 5X	3 μ L	98°C	3:00	98°C	2:00
Module 5'	X μ L	98°C	0:30	98°C	0:20
Module 3'	X μ L	56°C	0:30	62°C	0:20
<i>URA3</i>	X μ L	72°C	2:30	72°C	2:30
dNTP	1.5 μ L	4°C	1:00	72°C	3:30
iProof	0.3 μ L			12°C	1:00
Water	<u>3</u> μ L				
	15 μ L				

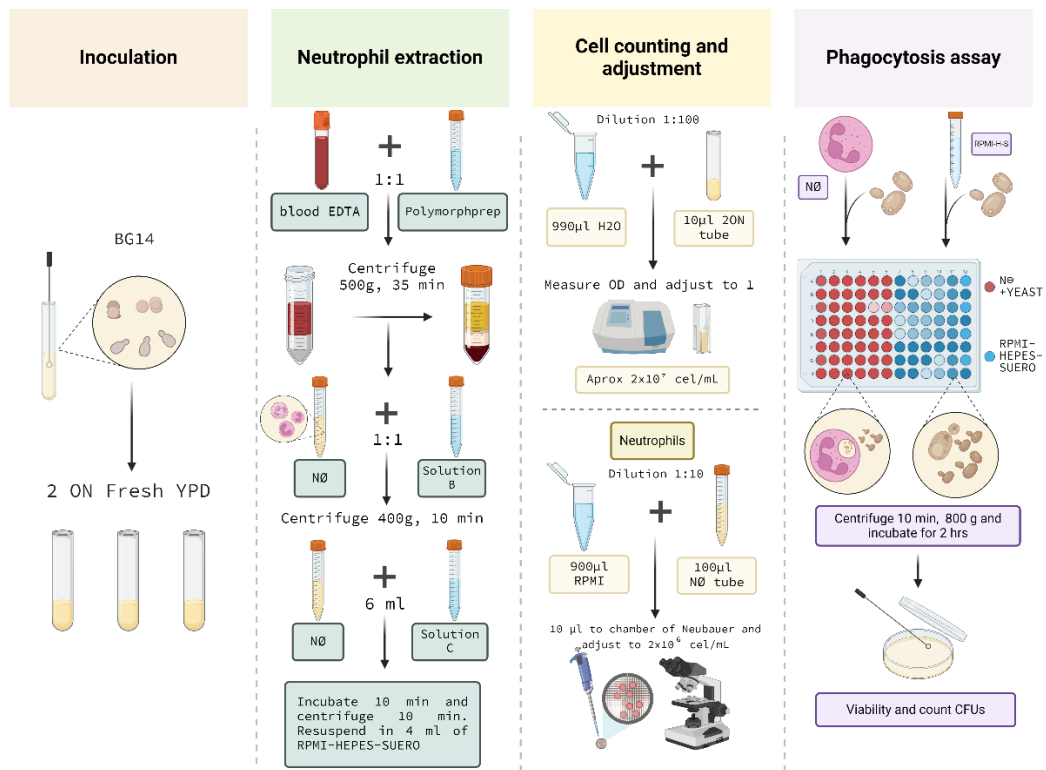
Buffer 5X	1 μ L				
#Prmer Fw	2 μ L				
#Primer Rv	<u>2</u> μ L				
	20 μ L				

739 **Table S4| Percent reversibility of Gly⁻ to Gly⁺ phenotype**

Strain	Parental	% of reversibility
5014	BG14	0%
5015	BG14	0%
5020	BG14	0%
5037	BG14	0%
5229	AN378	0%

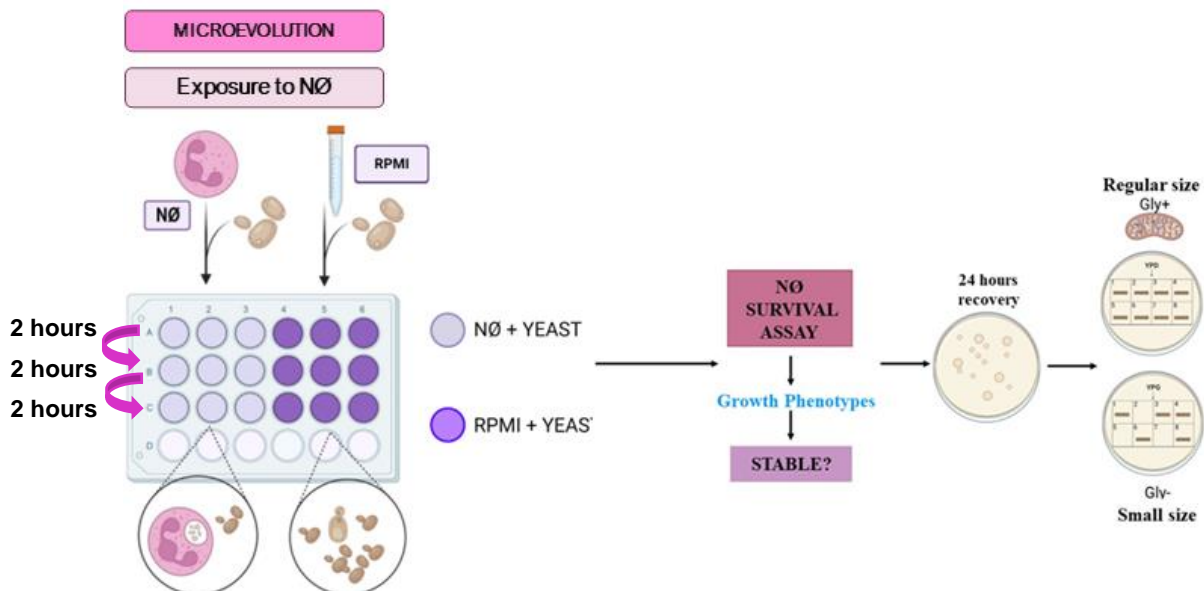
740

a)



742

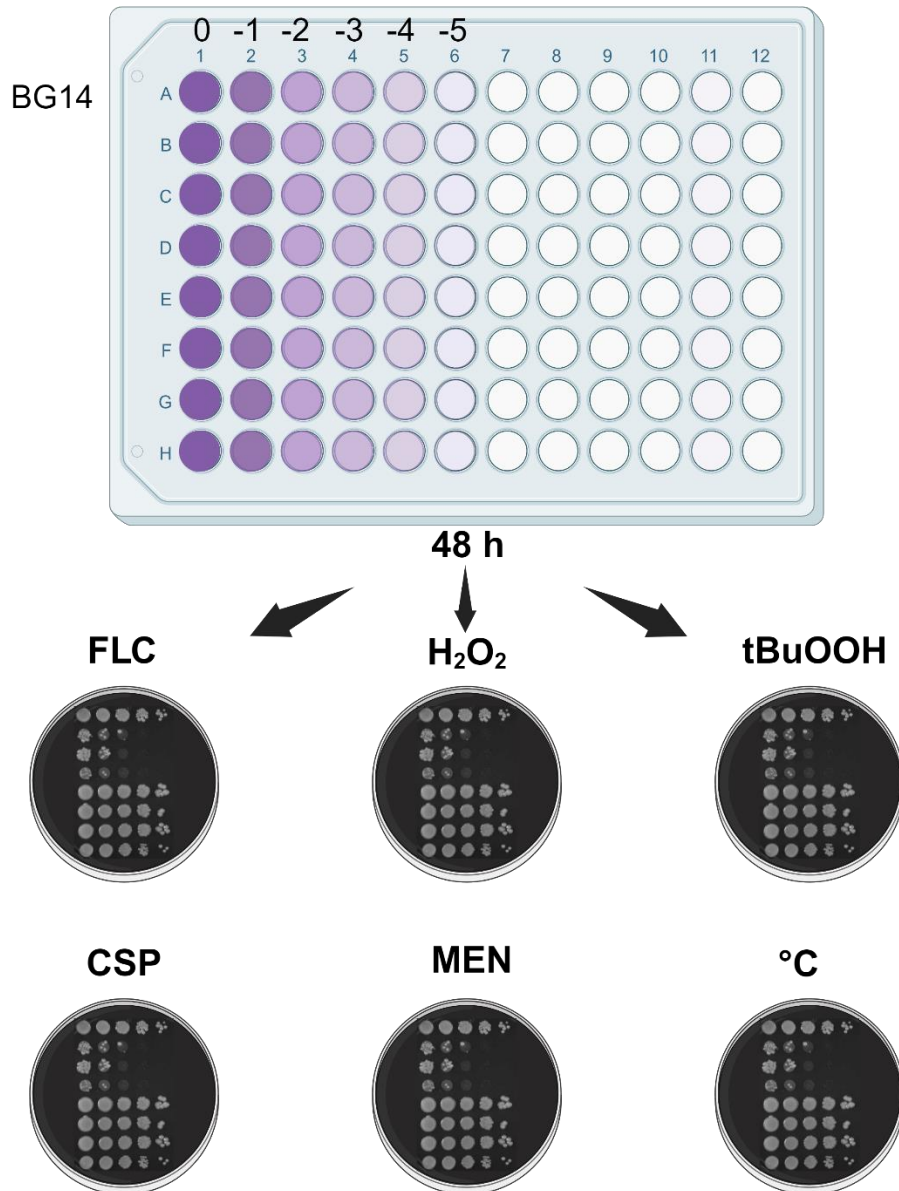
b)



743 **Fig. S1|Schematic representation of experimental approach.** Abbreviature:
 744 Optical density (OD), overnight (ON), water (H₂O), polymorphonuclear (PMN),
 745 colony-forming unit (CFU). a) Schematic representation of survival assay. b)
 746 Schematic representation of microevolution of *N. glabratus* cells.

747

Spott assay



748

749

Fig. S5| Schematic representation spot assay with different oxidant stresses,

750

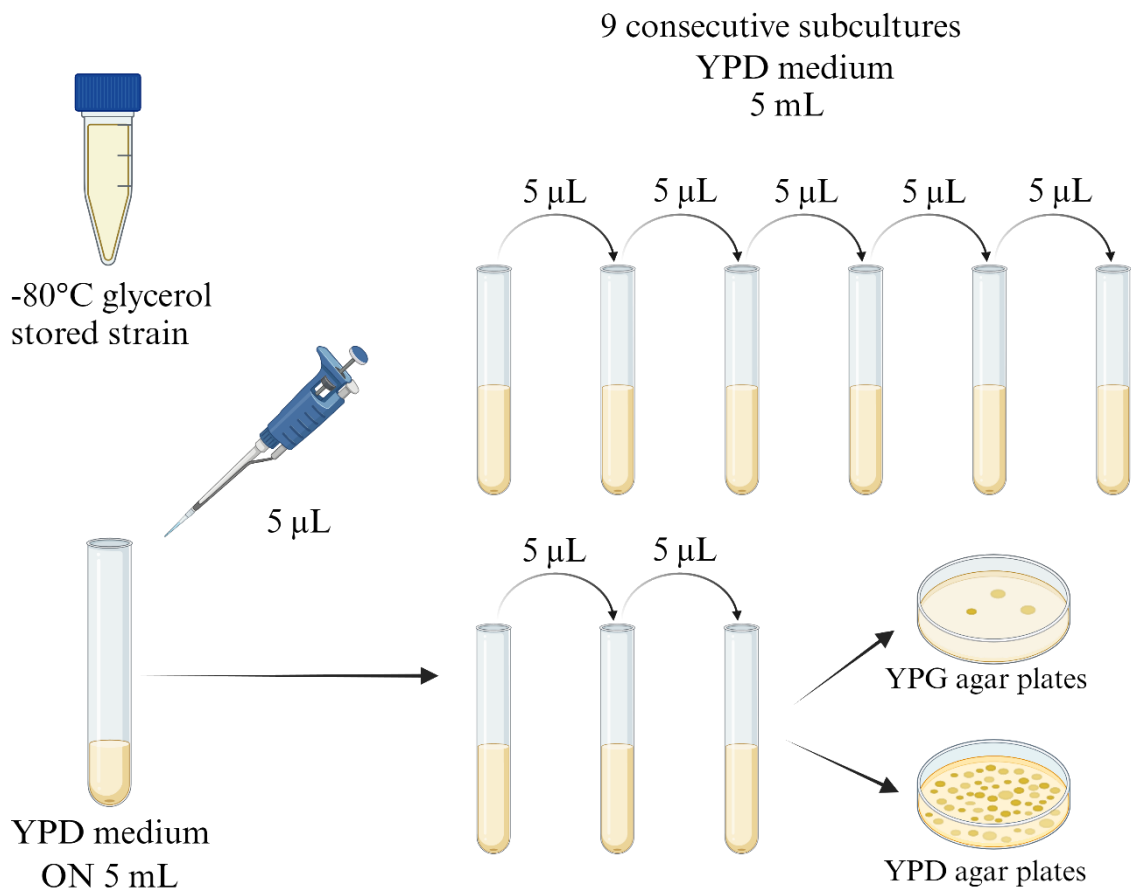
antifungals and thermal stress. Abbreviation: Fluconazole (FLC), Caspofungin

751

(CSP), Hydrogen peroxide (H₂O₂), Menadione (MEN), tert-butyl hydroperoxide

752

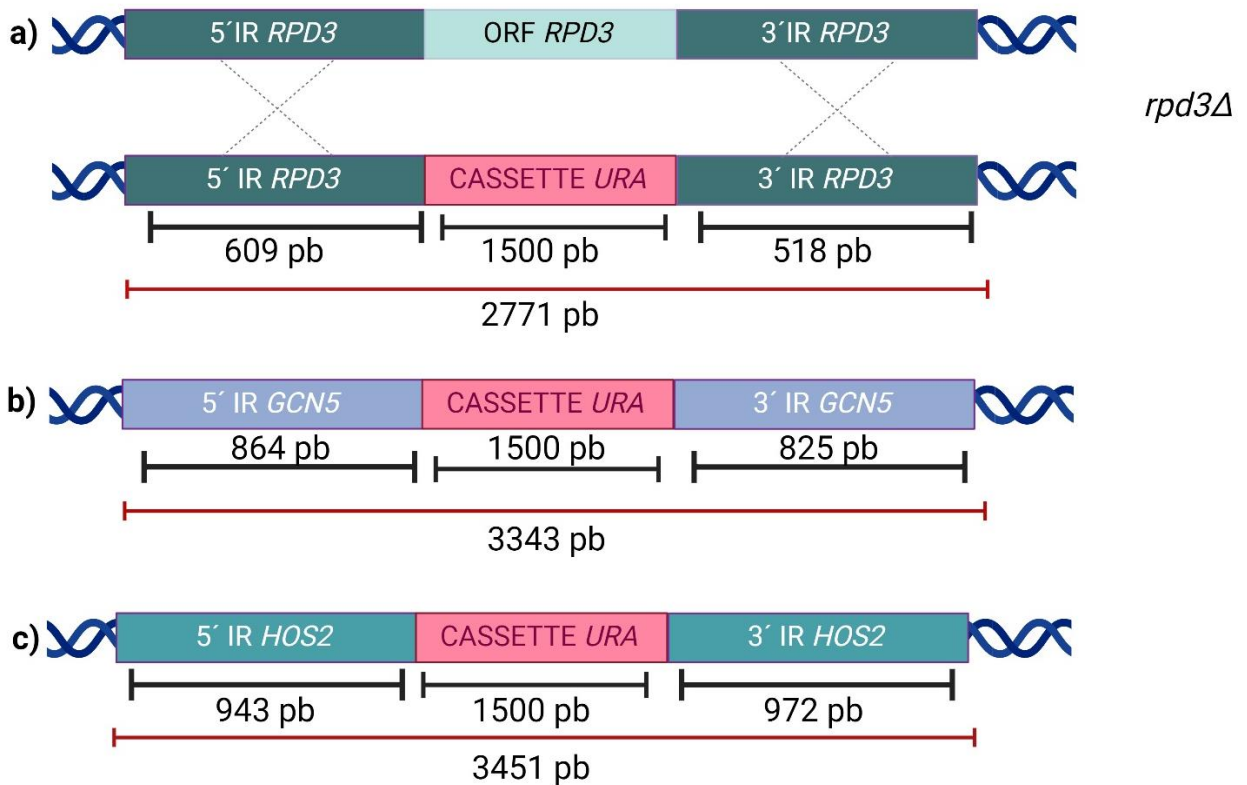
(tBuOOH), Temperature stress (°C).



753

754 **Fig. S6| Schematic representation of reversibility assay.**

755



756

Fig. S7| Schematic representation of the experimental approach of fusion PCR.

Abbreviation: IR: Intergenic region. a) *RPD3* ORF knockout replaced by *URA3* selection marker. b) *GCN5* ORF knockout replaced by *URA3* selection marker. c) *HOS2* ORF knockout replaced by *URA3* selection marker. All these knockout mutants were performed by a fusion PCR, which is caused by a homologous recombination event.